Received: 9 February 2021 | Revised: 13 December 2022 | Accepted: 14 March 2023

DOI: 10.1002/num.23021

RESEARCH ARTICLE

WILEY

On the numerical approximation of Boussinesq/Boussinesq systems for internal waves

Vassilios A. Dougalis[1,2] | **Angel Duran**[3] | **Leetha Saridaki**[1,2]

[1]Mathematics Department, University of Athens, Zografou, 15784, Greece
[2]Institute of Applied & Computational Mathematics, Foundation for Research and Technology-Hellas, Heraklion, 71110, Greece
[3]Applied Mathematics Department, University of Valladolid, Valladolid, 47011, Spain

Correspondence
Angel Duran, Applied Mathematics Department, University of Valladolid, 47011, Valladolid, Spain.
Email: angeldm@uva.es

Funding information
Agencia Estatal de Investigación, Grant/Award Number: PID2020-113554GB-I00/AEI/10.13039/501100011033; European Regional Development Fund, Grant/Award Numbers: NSRF 2014-2020, VA193P20, MIS5002358.

Abstract

The present paper is concerned with the numerical approximation of a three-parameter family of Boussinesq systems. The systems have been proposed as models of the propagation of long internal waves along the interface of a two-layer system of fluids with rigid-lid condition for the upper layer and under a Boussinesq regime for the flow in both layers. We first present some theoretical properties of the systems on well-posedness, conservation laws, Hamiltonian structure, and solitary-wave solutions, using the results for analogous models for surface wave propagation. Then the corresponding periodic initial-value problem is discretized in space by the spectral Fourier Galerkin method and for each system, error estimates for the semidiscrete approximation are proved. The spectral semidiscretizations are numerically integrated in time by a fourth-order Runge–Kutta-composition method based on the implicit midpoint rule. Numerical experiments illustrate the accuracy of the fully discrete scheme, in particular its ability to simulate accurately solitary-wave solutions of the systems.

KEYWORDS

Boussinesq/Boussinesq systems, error estimates, internal waves, solitary waves, spectral methods

This article is dedicated to the memory of Professor Dougalis

1 | INTRODUCTION

The following three-parameter family of Boussinesq/Boussinesq (B/B) systems for internal waves was derived by Bona et al. [7]:

$$\begin{aligned}&(1-b\Delta)\zeta_t+\frac{1}{\gamma+\delta}\nabla\cdot\mathbf{v}_\beta+\left(\frac{\delta^2-\gamma}{(\delta+\gamma)^2}\right)\nabla\cdot\left(\zeta\mathbf{v}_\beta\right)+a\nabla\cdot\Delta\mathbf{v}_\beta=0,\\&(1-d\Delta)(\mathbf{v}_\beta)_t+(1-\gamma)\nabla\zeta+\left(\frac{\delta^2-\gamma}{2(\delta+\gamma)^2}\right)\nabla|\mathbf{v}_\beta|^2+(1-\gamma)c\Delta\nabla\zeta=0.\end{aligned}\tag{1}$$

The system (1) is a model (in nondimensional, unscaled form) for the propagation of internal waves along the interface of an inviscid, homogeneous, two-layer system of fluids, the upper of which is labeled 1 and the lower 2. The layers have depths d_1, d_2 and densities ρ_1, ρ_2 with $\rho_2 > \rho_1$. The upper layer is restricted by the rigid-lid assumption, at depth $z = 0$, while the rigid, horizontal bottom lies at depth $z = -(d_1 + d_2)$. In (1) $\zeta = \zeta(x, y, t)$ represents the deviation of the interface from the rest position at (x, y) at time t, while $\mathbf{v}_\beta = (I - \beta\Delta)^{-1}\mathbf{v}$, where $\beta \geq 0$ is a modeling parameter, Δ denotes the Laplace operator and $\mathbf{v}$ is a "velocity" variable defined in [7] in terms of the horizontal components of the velocities of the two layers of fluids $\mathbf{v}^{(1)}$ and $\mathbf{v}^{(2)}$ as the difference $\mathbf{v}^{(2)} - \gamma\mathbf{v}^{(1)}$ evaluated at the interface. The constants

$$\gamma=\frac{\rho_1}{\rho_2}<1,\quad \delta=\frac{d_1}{d_2},$$

denote the density and depth ratios, respectively. The parameters a, b, c, d depend on the physical parameters δ, γ and the modeling parameters $\alpha_1 \geq 0, \beta \geq 0$ and $\alpha_2 \leq 1$ [7], and are given by

$$\begin{aligned}&a=\frac{(1-\alpha_1)(1+\gamma\delta)-3\delta\beta(\delta+\gamma)}{3\delta(\gamma+\delta)^2},\quad b=\alpha_1\frac{1+\gamma\delta}{3\delta(\gamma+\delta)},\\&c=\beta\alpha_2,\quad d=\beta(1-\alpha_2).\end{aligned}\tag{2}$$

These formulas lead to the relation

$$(\delta+\gamma)a+b+c+d=S(\gamma,\delta),\quad S(\gamma,\delta):=\frac{1+\gamma\delta}{3\delta(\gamma+\delta)}.\tag{3}$$

The case $\gamma = 0, \delta = 1$ corresponds to the Boussinesq systems for surface water waves analyzed by Bona, Chen, and Saut in [5, 6]. In that case β should be taken equal to $\frac{1}{2}(1-\theta^2)$ in the notation of [5, 6], where $0 \leq \theta \leq 1$ defines a parametrization of the depth variable $z = -1 + \theta$, ζ is the displacement of the surface elevation of the wave over the rest position $z = 0$, and the horizontal velocity at the free surface would be given by $\mathbf{v}$. The variable $\mathbf{v}_\beta$ represents now the horizontal velocity at depth $z = -1 + \theta$.

In [7] (see also [27]), several asymptotic models for internal waves in different physical regimes are derived, and the consistency of the corresponding full Euler equations with them is established in a rigorous manner. The physical regimes are defined in terms of the scaling parameters

$$\epsilon=\frac{a}{d_1},\quad \mu=\frac{d_1^2}{\lambda^2},\tag{4}$$

and δ, where a and λ denote a typical amplitude and wavelength of the interface wave, respectively. The parameters (4) are defined with respect to the upper layer; similar ones, ϵ_2 and μ_2, can be defined with respect to the lower layer. Then the system (1) is valid in the so-called B/B regime; this means that the flow is in the Boussinesq regime in both fluid domains, that is, the physical parameters satisfy the conditions $\delta \sim 1$ and

$$\mu\sim\mu_2\sim\epsilon\sim\epsilon_2\ll 1.$$

For a review of several other issues concerning the modeling of internal waves in the B/B and the other asymptotic regimes defined in [7] we refer the reader to the notes of Saut [27]. We would also like to mention that Nguyen and Dias derived in [24] a B/B system and extended it to the case of higher-power nonlinear terms. In [16] (see also references therein) Duchêne derived and studied some B/B models for internal waves in both the free-surface and rigid-lid cases. A KdV approximation is also proved and illustrated with some numerical comparisons for different initial data.

The present study is focused on the one-dimensional version of (1), which is written in unscaled, dimensionless variables, for $x \in \mathbb{R}, t \geq 0$, as

$$(1 - b\partial_{xx})\zeta_t + \frac{1}{\gamma + \delta}\partial_x v_\beta + \left(\frac{\delta^2 - \gamma}{(\delta + \gamma)^2}\right)\partial_x\left(\zeta v_\beta\right) + a\partial_{xxx}v_\beta = 0,$$
$$(1 - d\partial_{xx})(v_\beta)_t + (1 - \gamma)\partial_x\zeta + \left(\frac{\delta^2 - \gamma}{2(\delta + \gamma)^2}\right)\partial_x v_\beta^2 + (1 - \gamma)c\partial_{xxx}\zeta = 0, \tag{5}$$

with $v_\beta = (1 - \beta\partial_{xx})^{-1}u$.

The principal goal of this study is two-fold. In Section 2, we first study the linear and nonlinear well-posedness of the initial-value problem (IVP) of B/B systems for various values of the coefficients a, b, c, d, based on the analogous theory valid for the Boussinesq systems for surface waves presented in [5, 6]. We identify seven classes of B/B systems that are linearly well posed with coefficients relevant to the internal-wave problem and whose initial-value problems are nonlinearly, in general locally in time, well-posed in appropriate pairs of Sobolev spaces. In addition, other properties of (5) are discussed, namely the conservation of various quantities by the solutions and the Hamiltonian structure for some of the systems. The issue of existence of special solutions such as classical and generalized solitary waves is studied in detail theoretically and numerically in the companion paper [13], compare also [14], in which we examine the application to (5) of standard theories of existence of solitary waves, construct numerical approximations to the solitary-wave profiles, and study computationally properties of the dynamics of these solutions.

In the rest of the article, we consider in detail the numerical approximation of the well-posed systems of the family (5). Specifically, in Section 3 we discretize in space the periodic IVP for these systems using the spectral Fourier–Galerkin method and prove L^2 error estimates for the ensuing semidiscrete approximations. These estimates remain of course valid for the analogous surface-wave Boussinesq systems (take $\gamma = 0, \delta = 1$ in (5)).

In recent years there have appeared several papers with rigorous error estimates for numerical methods for surface-wave Boussinesq-type systems. For example, in [3, 4, 15, 31] one may find error analyses of Galerkin-Finite element semidiscretizations for various initial-boundary-value problems (IBVP's) for several Boussinesq systems in one and two space dimensions. The papers [3] and [4] also contain error estimates of temporal discretizations of the semidiscrete problems effected with high-order accurate, explicit Runge–Kutta (RK) time-stepping schemes. In [32] Xavier et al. analyze spectral methods of collocation type, coupled with the explicit, "classical," fourth-order accurate RK scheme for time-stepping for the surface-wave Boussinesq systems corresponding to the classes of the cases (i) and (v), compare Section 2.

We complete the study of the numerical approximation of (5) by integrating numerically in time the spectral semidiscrete systems using a fourth-order Runge–Kutta-composition method based on the implicit midpoint rule. For the case of spectral semidiscretizations of the periodic IVP of the Korteweg-de Vries (KdV) equation, an analysis of convergence of the full discretization with this method has been made in [9]. The scheme has also been shown to be efficient when approximating other nonlinear dispersive equations [12, 18]. Concerning the B/B systems (5), in Section 4 we formulate the corresponding fully discrete method and study computationally its performance by means of several numerical experiments. The method is used in the companion paper [13] to conduct a numerical study on the dynamics of solitary-wave solutions. Concluding remarks are outlined in Section 5. An extended version of the present paper and of [13] can be found in [14].

The following notation will be used throughout the article. For real s, $H^s(\mathbb{R})$ stands for the L^2-based Sobolev space over $\mathbb{R}$. On the interval $(0,1)$, the inner product on $L^2 = L^2(0,1)$ is denoted by $(\cdot,\cdot)$, and the corresponding norm by $\|\cdot\|$. For real $\mu \geq 0$ we denote the L^2-based periodic Sobolev spaces on $[0,1]$ by H^μ; for $g \in H^\mu$ its H^μ norm will be given by

$$\|g\|_\mu = \left(\sum_{k\in\mathbb{Z}} (1+k^2)^\mu |\widehat{g}(k)|^2 \right)^{1/2},$$

where $\widehat{g}(k)$ is the kth Fourier coefficient of g. We let $|\cdot|_\infty$ resp. $\|\cdot\|_{j,\infty}$ be the norm on L^∞, resp. $W^{j,\infty}$, on $(0,1)$, where for $1 \leq p \leq \infty$ $W^{\mu,p} = W^{\mu,p}(0,1)$ is the Sobolev space of periodic functions on $(0,1)$ of order μ, whose generalized derivatives are in L^p.

2 | DERIVATION AND WELL-POSEDNESS

In this section, we review results of linear and nonlinear well-posedness of the systems (5) based on the analogous theory of [5, 6] valid for surface-wave Boussinesq systems, note some invariant functionals of the solutions of these systems and make a brief introduction to the solitary-wave solutions thereof.

2.1 | Well-posedness theory

The associated to (5) linearized system, written in terms of ζ and $u = (I - \beta\partial_{xx})v_\beta$ is for $x \in \mathbb{R}, t \geq 0$ given by

$$\begin{aligned} (1 - b\partial_{xx})\zeta_t + \frac{1}{\gamma+\delta}\partial_x(I-\beta\partial_{xx})^{-1}u + a(1-\beta\partial_{xx})^{-1}\partial_{xxx}u &= 0, \\ (1-d\partial_{xx})(1-\beta\partial_{xx})^{-1}u_t + (1-\gamma)\partial_x\zeta + (1-\gamma)c\partial_{xxx}\zeta &= 0. \end{aligned} \tag{6}$$

The Fourier transform leads to the system

$$\frac{d}{dt}\begin{pmatrix} \widehat{\zeta}(k,t) \\ \widehat{u}(k,t) \end{pmatrix} + (ik)A(k)\begin{pmatrix} \widehat{\zeta}(k,t) \\ \widehat{u}(k,t) \end{pmatrix} = 0, \tag{7}$$

where $k \in \mathbb{R}, t \geq 0$, a circumflex denotes the Fourier transform, and

$$A(k) = \begin{pmatrix} 0 & \omega_1(k) \\ \omega_2(k) & 0 \end{pmatrix},$$

where

$$\omega_1(k) = \frac{\left(\frac{1}{\delta+\gamma} - ak^2\right)}{(1+bk^2)(1+\beta k^2)}, \quad \omega_2(k) = \frac{(1-\gamma)(1-ck^2)(1+\beta k^2)}{1+dk^2}.$$

The study of (6) (or (7)) can be done in a similar way to that of [5]. If

$$\omega_1(k)\omega_2(k) = \frac{\left(\frac{1}{\delta+\gamma} - ak^2\right)(1-\gamma)(1-ck^2)}{(1+bk^2)(1+dk^2)} \geq 0,$$

then the IVP for the linearized system (7) is well posed if the matrix

$$e^{-ikA(k)t} = \begin{pmatrix} \cos(k\sigma(k)t) & -i\frac{\omega_1(k)}{\sigma(k)}\sin(k\sigma(k)t) \\ -i\frac{\omega_2(k)}{\sigma(k)}\sin(k\sigma(k)t) & \cos(k\sigma(k)t) \end{pmatrix},$$

where $\sigma = \sqrt{\omega_1\omega_2}$, has elements which are bounded for bounded intervals of k. This holds when ω_1/ω_2 has neither poles nor zeros on the real axis. Since

$$\frac{\omega_1(k)}{\omega_2(k)} = \frac{\left(\frac{1}{\delta+\gamma} - ak^2\right)(1+dk^2)}{(1+\beta k^2)^2(1-\gamma)(1-ck^2)(1+bk^2)},$$

and $\beta \geq 0, 0 < \gamma < 1$ and $\delta > 0$, this is equivalent to requiring that the rational function

$$\frac{\left(\frac{1}{\delta+\gamma} - ak^2\right)(1+dk^2)}{(1-ck^2)(1+bk^2)},$$

have no poles nor zeros for $k \in \mathbb{R}$. This leads to the three "admissible" cases,

(C1) $a, c \leq 0, b, d \geq 0$.
(C2) $b, d \geq 0, c = a(\delta+\gamma) > 0$.
(C3) $b = d < 0, c = a(\delta+\gamma) > 0$.

We note that

$$\alpha_1 = \frac{3\delta(\delta+\gamma)}{1+\gamma\delta}b, \quad \beta = c+d, \quad \alpha_2 = \frac{c}{c+d},$$

and observe that (C3) does not satisfy the hypotheses

$$\alpha_2 \leq 1, \quad \alpha_1 \geq 0.$$

On the other hand, the case (C2) requires

$$0 < \alpha_1 < 1, \quad 0 < \alpha_2 \leq 1, \quad \beta > 0.$$

In the present paper only the case (C1) will be considered.

If we recall that the order of $\sigma(k)$ is the integer l such that

$$\sigma(k) \approx |k|^l, \quad |k| \to \infty,$$

then Theorem 3.2 of [5] can be applied to prove that if $m_1 = \max\{0, -l\}, m_2 = \max\{0, l\}$ then the IVP for the linear system (6) is well posed for (ζ, u) in $H^{s+m_1}(\mathbb{R}) \times H^{s+m_2}(\mathbb{R})$ for any $s \geq 0$. As already mentioned, the case $\beta = 0$ leads to conditions for the linear well-posedness for Boussinesq systems for surface waves [5].

Remark 1. It is to be noted that not all cases described by the set $a, c \leq 0, b, d \geq 0$ are relevant for the internal wave problem, due to the restrictions on the physical parameters γ, δ and the modeling parameters, $\alpha_1, \alpha_2, \beta$ that determine a, b, c, and d, compare (2) and (3). Specifically, the case $a = 0, c < 0, b > 0, d = 0$ should be excluded since $d = 0$ implies either $\beta = 0$ or $\alpha_2 = 1$ and in either case $c < 0$ cannot hold. Arguing similarly we may see that all cases with $b = d = 0, a, c \leq 0$ are not valid for internal waves. In addition, note that several other cases hold, under easily checked conditions between the parameters. (For example, if two of the four parameters are zero, then (3) implies an affine relation between the other two.)

As far as local in time well-posedness of the full nonlinear system is concerned, the analysis made in [6] for the case of surface waves can also be used here. (This was confirmed in [2].) Let us consider the systems corresponding to those cases among the set of parameters $b, d \geq 0, a, c \leq 0$ that are relevant for internal waves. In each case of the following list, we mention the corresponding theorem of [6] that applies. All the results concern existence, uniqueness, and regularity locally in t of the corresponding solution in the appropriate pairs of Sobolev spaces shown.

- Case (i): $b, d > 0, a = c = 0$ (systems of "BBM-BBM" type; Theorem 2.1, $H^s(\mathbb{R}) \times H^s(\mathbb{R})$, $s \geq 0$).
- Case (ii): $b, d > 0, a, c < 0$ ("generic" case; Theorem 2.5, $H^s(\mathbb{R}) \times H^s(\mathbb{R}), s \geq 0$).
- Case (iii): $b = 0, d > 0, a, c < 0$ (Theorem 3.5, $H^s(\mathbb{R}) \times H^{s+1}(\mathbb{R}), s \geq 1$).
- Case (iv): $b = 0, d > 0, a = c = 0$ ("classical" Boussinesq system; Theorem 3.3, $H^s(\mathbb{R}) \times H^{s+1}(\mathbb{R}), s \geq 1$, conditional global existence; see also [17]), or $b > 0, d = 0, a = c = 0$ (analogous theory).
- Case (v): $b, d > 0, a = 0, c < 0$ (Bona-Smith system; Theorem 2.6, $H^{s+1}(\mathbb{R}) \times H^s(\mathbb{R}), s \geq 0$, conditional global existence), or $b, d > 0, a < 0, c = 0$ (analogous theory).
- Case (vi): $b = 0, d > 0, a < 0, c = 0$ (Theorem 3.1, $H^s(\mathbb{R}) \times H^{s+2}(\mathbb{R}), s \geq 1$).
- Case (vii): $b > 0, d = 0, a < 0, c = 0$ (Theorem 3.9, $H^s(\mathbb{R}) \times H^s(\mathbb{R}), s \geq 2$) or $b = 0, d > 0, a = 0, c < 0$ (analogous theory).

Note that slightly sharper regularity results were achieved in [2] for some of these cases.

2.2 | Conserved quantities

It is not hard to show that the linear functionals

$$M_1(\zeta) = \int_{-\infty}^{\infty} \zeta dx, \quad M_2(v_\beta) = \int_{-\infty}^{\infty} v_\beta dx = \int_{-\infty}^{\infty} (1 - \beta\partial_{xx})^{-1} u dx,$$

are invariant quantities during the evolution of suitable solutions of (5). When $b = d$ (cf. the surface wave case [6]) we have the conserved functionals

$$I(\zeta, u) = \int_{-\infty}^{\infty} (\zeta v_\beta + b\partial_x\zeta\partial_x v_\beta) dx, \tag{8}$$

$$H(\zeta, u) = \int_{-\infty}^{\infty} \left(\frac{(1-\gamma)}{2}\zeta^2 + \frac{1}{2(\delta+\gamma)} v_\beta^2 - a(\partial_x v_\beta)^2 - (1-\gamma)c(\partial_x\zeta)^2 + \frac{\delta^2 - \gamma}{2(\delta+\gamma)^2}\zeta v_\beta^2 \right) dx, \tag{9}$$

(where $v_\beta = (1 - \beta\partial_{xx})^{-1}u$) with the Hamiltonian structure for (5) given by

$$\frac{d}{dt}\begin{pmatrix} \zeta \\ u \end{pmatrix} = J\frac{\delta H}{\delta(\zeta, u)},$$

$$J = -\partial_x(1 - \beta\partial_{xx})^{-1} \begin{pmatrix} (1 - b\partial_{xx}) & 0 \\ 0 & (1 - d\partial_{xx}) \end{pmatrix} \begin{pmatrix} 0 & -1 \\ 1 & 0 \end{pmatrix}, \tag{10}$$

where $\delta H/\delta(\zeta, u)$ stands for the variational derivative with respect to the variables (ζ, u). All these conservation laws as well as the Hamiltonian structure hold in suitable function spaces.

2.3 | Solitary-wave solutions

An important property of the systems (5) is that they possess solitary-wave solutions. These are solutions of (5) of the form $\zeta = \zeta(x - c_s t), u = u(x - c_s t)$ that satisfy

$$\partial_x \begin{pmatrix} c_s(1 - b\partial_{xx}) & -\frac{1}{\delta+\gamma} - a\partial_{xx} \\ -(1-\gamma)(1 + c\partial_{xx}) & c_s(1 - d\partial_{xx}) \end{pmatrix} \begin{pmatrix} \zeta \\ v_\beta \end{pmatrix} = \kappa_{\gamma,\delta}\partial_x \begin{pmatrix} \zeta v_\beta \\ \frac{v_\beta^2}{2} \end{pmatrix}, \tag{11}$$

where $\kappa_{\gamma,\delta} = \frac{\delta^2-\gamma}{(\delta+\gamma)^2}$. That is, they are waves of permanent form traveling with speed $c_s \neq 0$. As mentioned in Section 1, in the companion paper [13] we study the existence, numerical generation and dynamics of these solutions (see also [14]). The family of B/B systems (5) has two different types of solitary-wave solutions. If we consider (11) as a dynamical system, the profiles ζ and u could be orbits homoclinic to the origin at infinity ($\zeta, u \to 0$ as $|x - c_s t| \to \infty$), and therefore will be solutions of the system

$$\begin{pmatrix} c_s(1 - b\partial_{xx}) & -\frac{1}{\delta+\gamma} - a\partial_{xx} \\ -(1-\gamma)(1 + c\partial_{xx}) & c_s(1 - d\partial_{xx}) \end{pmatrix} \begin{pmatrix} \zeta \\ v_\beta \end{pmatrix} = \kappa_{\gamma,\delta} \begin{pmatrix} \zeta v_\beta \\ \frac{v_\beta^2}{2} \end{pmatrix}. \tag{12}$$

The corresponding solutions of (5) are then classical solitary waves. In addition, there exist generalized solitary waves, which are solutions of (5) whose profiles ζ and u satisfy (12) and are homoclinic to periodic orbits at infinity [21-23]. The existence of both types of solitary-wave solutions is studied in [13] (see also [14]).

3 | ERROR ESTIMATES FOR A SPECTRAL SEMIDISCRETIZATION OF THE PERIODIC INITIAL-VALUE PROBLEM

We consider the periodic IVP for the one-dimensional system (5) on the spatial interval $[0, 1]$. In order to simplify notation we denote $v_\beta = u, \lambda = \kappa_{\gamma,\delta} = \frac{\delta^2-\gamma}{(\delta+\gamma)^2}, \kappa_1 = \frac{1}{\delta+\gamma}, \kappa_2 = 1 - \gamma$. (Thus κ_1 and κ_2 are positive constants.) We also let c' denote the constant $(1-\gamma)c$ multiplying the term $\partial_{xxx}\zeta$ in the second pde of (5); this does not change the sign of the original c. Thus, given $u_0(x), \zeta_0(x)$, 1-periodic real functions, we seek for $0 \leq t \leq T, \zeta(x,t), u(x,t)$, 1-periodic in x, satisfying, for $0 \leq x \leq 1$, $0 \leq t \leq T$

$$\begin{aligned} \zeta_t + \kappa_1 u_x + \lambda (\zeta u)_x + a u_{xxx} - b\zeta_{xxt} &= 0, \\ u_t + \kappa_2 \zeta_x + \lambda u u_x + c'\zeta_{xxx} - d u_{xxt} &= 0, \end{aligned} \tag{13}$$

with

$$\zeta(x,0) = \zeta_0(x),\ u(x,0) = u_0(x),\ 0 \leq x \leq 1. \tag{14}$$

In the sequel we assume that the IVP (13), (14) has a unique solution which is smooth enough for the purposes of error estimation.

We will discretize (13), (14) in space by a spectral Fourier Galerkin method. To this end we let $N \geq 1$ be an integer and define the finite dimensional space S_N as

$$S_N = \text{span}\{e^{2\pi ikx},\ k \in \mathbb{Z}, -N \leq k \leq N\}.$$

Let $P = P_N$ denote the L^2-projection operator onto S_N given explicitly for $v \in L^2$ by

$$Pv = \sum_{|k|\leq N} \hat{v}(k)e^{2\pi ikx},$$

where $\widehat{v}(k)$ is the kth Fourier coefficient of v. It is obvious that P commutes with ∂_x. Moreover, given integers $0 \le j \le \mu$, there exists a constant C independent of N, such that for any $v \in H^\mu$,

$$\|v - Pv\|_j \le CN^{j-\mu}\|v\|_\mu, \ \mu \ge 0, \tag{15}$$

$$|v - Pv|_\infty \le CN^{1/2-\mu}\|v\|_\mu, \ \mu \ge 1. \tag{16}$$

In addition, the following inverse inequalities hold in S_N: Given $0 \le j \le \mu$, there exists a constant C independent of N, such that for any $\psi \in S_N$

$$\|\psi\|_\mu \le CN^{\mu-j}\|\psi\|_j, \ \|\psi\|_{\mu,\infty} \le CN^{1/2+\mu-j}\|\psi\|_j. \tag{17}$$

In what follows, as is customary, we will denote constants independent of N by C.

The spectral Galerkin semidiscretization of the IVP (13), (14) is defined as follows. Let $T > 0$. We seek real-valued $\zeta_N, u_N : [0, T] \to S_N$ satisfying for $0 \le t \le T$ and $\forall \varphi, \chi \in S_N$

$$(\zeta_{Nt}, \varphi) + \kappa_1(u_{Nx}, \varphi) + \lambda((\zeta_N u_N)_x, \varphi) + a(u_{Nxxx}, \varphi) - b(\zeta_{Nxxt}, \varphi) = 0, \tag{18}$$

$$(u_{Nt}, \chi) + \kappa_2(u_{Nx}, \chi) + \lambda(u_N u_{Nx}, \chi) + c'(\zeta_{Nxxx}, \chi) - d(u_{Nxxt}, \chi) = 0, \tag{19}$$

and for $t = 0$

$$\zeta_N(0) = P\zeta_0, \ u_N(0) = Pu_0. \tag{20}$$

The ODE IVP (18)–(20) has a unique solution locally in time and a Fourier implementation

$$\begin{aligned} &(1 + bk^2)\widehat{\zeta}_{N,t} + ik\kappa_1\widehat{u}_N + ik\lambda\widehat{\zeta_N u_N} - ik^3 a\widehat{u}_N = 0, \\ &(1 + dk^2)\widehat{u}_{N,t} + ik\kappa_2\widehat{\zeta}_N + \frac{ik}{2}\lambda\widehat{u_N^2} - ik^3 c'\widehat{\zeta}_N = 0, \end{aligned} \tag{21}$$

where $\widehat{\zeta}_N = \widehat{\zeta}_N(k,t), \widehat{u}_N = \widehat{u}_N(k,t), -N \le k \le N, t \ge 0$ are the Fourier coefficients of ζ_N, u_N with initial values $\widehat{\zeta}_N(k,0) = \widehat{\zeta}_0(k), \widehat{u}_N(k,0) = \widehat{u}_0(k)$.

In order to estimate the error of the semidiscretization let $\theta = \zeta_N - P\zeta, \rho = P\zeta - \zeta$, so that $\zeta_N - \zeta = \theta + \rho$, and $\xi = u_N - Pu, \sigma = Pu - u$, so that $u_N - u = \xi + \sigma$. Then, subtracting the first pde in (13) from (18) we obtain, while the solution of (18)–(20) exists and for all $\varphi \in S_N$

$$(\theta_t, \varphi) + \kappa_1(\xi_x, \varphi) + a(\xi_{xxx}, \varphi) - b(\theta_{xxt}, \varphi) = -\lambda((\zeta_N u_N)_x, \varphi) + \lambda((\zeta u)_x, \varphi).$$

Therefore for $\varphi \in S_N$

$$(\theta_t, \varphi) + a(\xi_{xxx}, \varphi) - b(\theta_{xxt}, \varphi) = -\kappa_1(\xi_x, \varphi) - (A_x, \varphi), \tag{22}$$

where

$$A = \lambda(\zeta_N u_N - \zeta u) = \lambda\left((\zeta + \theta + \rho)(u + \xi + \sigma) - \zeta u\right),$$

that is,

$$A = \lambda\left(u\rho + \zeta\sigma + u\theta + \zeta\xi + \sigma\theta + \rho\xi + \rho\sigma + \theta\xi\right). \tag{23}$$

Subtracting the second pde in (13) from (19) we get for $\chi \in S_N$

$$(\xi_t, \chi) + \kappa_2(\theta_x, \chi) + c'(\theta_{xxx}, \chi) - d(\xi_{xxt}, \chi) = -\lambda(u_N u_{Nx}, \chi) + \lambda(uu_x, \chi).$$

Therefore, for $\chi \in S_N$

$$(\xi_t, \chi) + c'(\theta_{xxx}, \chi) - d(\xi_{xxt}, \chi) = -\kappa_2(\theta_x, \chi) - (B_x, \chi), \tag{24}$$

where

$$B = \lambda\left(u\sigma + u\xi + \sigma\xi + \frac{1}{2}(\sigma^2 + \xi^2)\right). \tag{25}$$

Using the error equations (22)–(25) we proceed now to derive error estimates for the semidiscrete schemes (18)–(20).

For the purpose of the error analysis, we consider the same seven cases of nonlinearly well posed systems identified in Section 2.1. For simplicity, in the cases (iv), (v), and (vii) the following systems will be analyzed; the others are similar:

- Case (iv): "Classical Boussinesq" case: $b = 0, d > 0, a = c = 0$.
- Case (v): "Bona-Smith" systems: $b, d > 0, a = 0, c < 0$.
- Case (vii): $b > 0, d = 0, a < 0, c = 0$.

As mentioned in Section 1, the systems of cases (i) (BBM-BBM) and (v) ("Bona-Smith") have been discretized by a collocation spectral method in space and analyzed by Xavier et al. [32], in the case of surface waves. The error estimates obtained in [32] are similar to those that we obtain below for the spectral Galerkin method in these cases but we include the proofs as our techniques are somewhat different.

In all propositions below we assume for simplicity that $\zeta, u \in C^1(0, T, H^\mu)$, $\mu \geq 1$, and specify in each case the least integer μ needed for the validity of the error estimates. In all cases it is clear that ζ_N, u_N satisfy (18)–(20) at least locally in t; part of the proof is checking that they exist uniquely and satisfy (18)–(19) up to $t = T$.

Proposition 2. *Let a, b, c, d as in case (i). If $\mu \geq 1$ then*

$$\max_{0\leq t\leq T} (\|\zeta_N - \zeta\| + \|u_N - u\|) \leq CN^{-\mu}. \tag{26}$$

Proof. While the semidiscrete solution ζ_N, u_N exists, putting $\varphi = \theta$ in (22), $\chi = \xi$ in (24), using integration by parts and adding the resulting equations give

$$\frac{1}{2}\frac{d}{dt}\left(\|\theta\|^2 + \|\xi\|^2 + b\|\theta_x\|^2 + d\|\xi_x\|^2\right) = \kappa_1(\xi, \theta_x) + \kappa_2(\theta, \xi_x) + (A, \theta_x) + (B, \xi_x). \tag{27}$$

We estimate as follows the various terms in the right-hand side of (27). First

$$|(\xi, \theta_x)| \leq \|\xi\|\|\theta_x\| \leq \frac{1}{2}\left(\|\xi\|^2 + \|\theta_x\|^2\right). \tag{28}$$

For the various terms of (A, θ_x) we first see, using (15),

$$|(u\rho, \theta_x)| \leq |u|_\infty\|\rho\|\|\theta_x\| \leq C\left(N^{-2\mu} + \|\theta_x\|^2\right). \tag{29}$$

Similarly,

$$|(\zeta\sigma, \theta_x)| \leq |\zeta|_\infty\|\sigma\|\|\theta_x\| \leq C\left(N^{-2\mu} + \|\theta_x\|^2\right). \tag{30}$$

Now

$$|(u\theta, \theta_x)| \leq |u|_\infty\|\theta\|\|\theta_x\| \leq C\|\theta\|_1^2, \tag{31}$$

$$|(\zeta\xi, \theta_x)| \leq |\zeta|_\infty\|\xi\|\|\theta_x\| \leq C(\|\xi\|^2 + \|\theta_x\|^2). \tag{32}$$

Using (16) we see that $|\sigma|_\infty \leq C$ and therefore

$$|(\sigma\theta, \theta_x)| \leq |\sigma|_\infty\|\theta\|\|\theta_x\| \leq C\|\theta\|_1^2. \tag{33}$$

Similarly,

$$|(\rho\xi, \theta_x)| \leq |\rho|_\infty\|\xi\|\|\theta_x\| \leq C(\|\xi\|^2 + \|\theta_x\|^2), \tag{34}$$

$$|(\rho\sigma,\theta_x)| \le |\rho|_\infty \|\sigma\|\|\theta_x\| \le C(N^{-2\mu} + \|\theta_x\|^2). \tag{35}$$

Since $\theta(0) = 0$, using continuity, let $t_N, 0 < t_N \le T$, be the maximal time for which the solution of (18)–(20) exists and satisfies

$$|\theta|_\infty \le 1,\ 0 \le t \le t_N. \tag{36}$$

Then for $0 \le t \le t_N$

$$|(\theta\xi,\theta_x)| \le |\theta|_\infty \|\xi\|\|\theta_x\| \le \|\xi\|\|\theta_x\| \le \frac{1}{2}(\|\xi\|^2 + \|\theta_x\|^2). \tag{37}$$

From (29)–(37) we have therefore for $0 \le t \le t_N$ that

$$|(A,\theta_x)| \le C\left(N^{-2\mu} + \|\xi\|^2 + \|\theta\|_1^2\right). \tag{38}$$

For the rest of the terms on the right-hand side of (27) we first note that

$$|(\theta,\xi_x)| \le \|\theta\|\|\xi_x\| \le \frac{1}{2}\left(\|\theta\|^2 + \|\xi_x\|^2\right). \tag{39}$$

For the (B,ξ_x) terms, in view of (25) we have the following estimates. Note that by (15)

$$|(u\sigma,\theta_x)| \le |u|_\infty \|\sigma\|\|\theta_x\| \le C\left(N^{-2\mu} + \|\theta_x\|^2\right). \tag{40}$$

In addition,

$$|(u\xi,\xi_x)| \le |u|_\infty \|\xi\|\|\xi_x\| \le C\|\xi\|_1^2. \tag{41}$$

By (16)

$$|(\sigma\xi,\xi_x)| \le |\sigma|_\infty \|\xi\|\|\xi_x\| \le C\|\xi\|_1^2. \tag{42}$$

By (15), (16)

$$\left|\frac{1}{2}(\sigma^2,\xi_x)\right| \le \frac{1}{2}|\sigma|_\infty \|\sigma\|\|\xi_x\| \le C(N^{-2\mu} + \|\xi_x\|^2). \tag{43}$$

And finally, by periodicity,

$$\frac{1}{2}(\xi^2,\xi_x) = 0. \tag{44}$$

We conclude from (40)–(44) that, as long as the semidiscrete solution exists,

$$|(B,\xi_x)| \le C\left(N^{-2\mu} + \|\theta\|^2 + \|\xi\|_1^2\right). \tag{45}$$

Hence, since $b, d > 0$ we get from (27), (28), (38), (39), (45) that

$$\frac{d}{dt}\left(\|\theta\|_1^2 + \|\xi\|_1^2\right) \le C\left(N^{-2\mu} + \|\theta\|_1^2 + \|\xi\|_1^2\right),\ 0 \le t \le t_N.$$

Hence, by Gronwall's lemma and (20) we conclude that for $0 \le t \le t_N$ and for some constant $C = C(T)$ there holds

$$\|\theta\|_1 + \|\xi\|_1 \le CN^{-\mu}. \tag{46}$$

Therefore, since $|\theta|_\infty \le C\|\theta\|_1$ by Sobolev's theorem, we conclude by (46) and our hypothesis on μ that (for N sufficiently large) t_N was not maximal in (36). Arguing in the customary way we see that t_N may be taken equal to T, and (46) holds for $0 \le t \le T$. By (15) we conclude that (26) holds, so that ζ_N, u_N satisfy optimal-order error estimates in L^2, where by "optimal-order" in the context of spectral methods we mean that the semidiscrete approximations satisfy estimates like (15) if $\zeta, u \in H^\mu$. ■

Proposition 3. *Let a, b, c, d as in case (ii). If $\mu \geq 1$ then*

$$\max_{0\leq t\leq T} (\|\zeta_N - \zeta\| + \|u_N - u\|) \leq CN^{-\mu}.$$

Proof. While the semidiscrete solution ζ_N, u_N exists, putting $\varphi = \theta$ in (22), $\chi = \xi$ in (24) we obtain, using integration by parts, that

$$\frac{1}{2}\frac{d}{dt}\left(\|\theta\|^2 + b\|\theta_x\|^2\right) - a(\xi_{xx}, \theta_x) = \kappa_1(\xi, \theta_x) + (A, \theta_x), \tag{47}$$

$$\frac{1}{2}\frac{d}{dt}\left(\|\xi\|^2 + d\|\xi_x\|^2\right) + c'(\theta_x, \xi_{xx}) = \kappa_2(\theta, \xi_x) + (B, \xi_x). \tag{48}$$

Multiplying (47) by $-c'$ and (48) by $-a$ and adding the resulting equations we get

$$\frac{1}{2}\frac{d}{dt}\left(|c'|\|\theta\|^2 + |a|\|\xi\|^2 + b|c'|\|\theta_x\|^2 + d|a|\|\xi_x\|^2\right) = -c'\kappa_1(\xi, \theta_x)$$
$$- c'(A, \theta_x) - a\kappa_2(\theta, \xi_x) - a(B, \xi_x).$$

The rest of the proof proceeds exactly along the lines of that of Proposition 2. ∎

Proposition 4. *Let a, b, c, d as in case (iii). If $\mu > 3/2$ then*

$$\max_{0\leq t\leq T} (\|\zeta_N - \zeta\| + \|u_N - u\|_1) \leq CN^{1-\mu}. \tag{49}$$

Proof. While the semidiscrete solution ζ_N, u_N exists, putting $\varphi = \theta$ in (22), $\chi = \xi$ in (24) we obtain, using integration by parts, that

$$\frac{1}{2}\frac{d}{dt}\|\theta\|^2 - a(\xi_{xx}, \theta_x) = -\kappa_1(\xi_x, \theta) - (A_x, \theta), \tag{50}$$

$$\frac{1}{2}\frac{d}{dt}\left(\|\xi\|^2 + d\|\xi_x\|^2\right) + c'(\theta_x, \xi_{xx}) = \kappa_2(\theta, \xi_x) + (B, \xi_x). \tag{51}$$

Multiplying (50) by $-c'$ and (51) by $-a$ and adding the resulting equations gives

$$\frac{1}{2}\frac{d}{dt}\left(|c'|\|\theta\|^2 + |a|\|\xi\|^2 + d|a|\|\xi_x\|^2\right) = c'\kappa_1(\xi_x, \theta) + c'(A_x, \theta)$$
$$- a\kappa_2(\theta, \xi_x) - a(B, \xi_x). \tag{52}$$

We estimate the terms of the right-hand side of the above. Obviously,

$$|(\xi_x, \theta)| \leq \|\xi_x\|\|\theta\| \leq \frac{1}{2}\left(\|\theta\|^2 + \|\xi_x\|^2\right). \tag{53}$$

For the terms of (A_x, θ), using (23) and (15) and the fact that H^1 is an algebra, we have

$$|((u\rho)_x, \theta)| \leq \|u\rho\|_1\|\theta\| \leq C\|u\|_1\|\rho\|_1\|\theta\| \leq C\left(N^{2(1-\mu)} + \|\theta\|^2\right).$$

Similarly,

$$|((\zeta\sigma)_x, \theta)| \leq C\left(N^{2(1-\mu)} + \|\theta\|^2\right). \tag{54}$$

Using integration by parts we have

$$|((u\theta)_x, \theta)| = |\frac{1}{2}|(u_x\theta, \theta)| \leq C|u_x|_\infty\|\theta\|^2 \leq C\|\theta\|^2. \tag{55}$$

Also

$$|((\zeta\xi)_x, \theta)| \leq C\|\zeta\|_1\|\xi\|_1\|\theta\| \leq C\left(\|\xi\|_1^2 + \|\theta\|^2\right). \tag{56}$$

Using integration by parts and (16) and our hypothesis on μ

$$|((\sigma\theta)_x,\theta)| = \frac{1}{2}|(\sigma_x\theta,\theta)| \leq C|\sigma_x|_\infty\|\theta\|^2 \leq C\|\theta\|^2. \tag{57}$$

By (15)

$$|((\rho\xi)_x,\theta)| \leq C\|\rho\|_1\|\xi\|_1\|\theta\| \leq C\left(\|\xi\|_1^2 + \|\theta\|^2\right). \tag{58}$$

By (15), (16), and our hypothesis on μ

$$\begin{aligned}|((\rho\sigma)_x,\theta)| &\leq |\rho|_\infty\|\sigma_x\|\|\theta\| + |\sigma|_\infty\|\rho_x\|\|\theta\| \\ &\leq CN^{\frac{3}{2}-2\mu}\|\theta\| \leq CN^{-\mu}\|\theta\| \\ &\leq C\left(N^{-2\mu} + \|\theta\|^2\right).\end{aligned} \tag{59}$$

Now, since $\theta(0) = 0$, using continuity, let t_N, $0 < t_N \leq T$, be the maximal value of t for which the solution of (18)–(20) exists and satisfies

$$|\theta|_\infty \leq 1,\ 0 \leq t \leq t_N. \tag{60}$$

By (60) we have for $0 \leq t \leq t_N$, using integration by parts

$$\begin{aligned}|((\theta\xi)_x,\theta)| &= \frac{1}{2}|(\xi_x\theta,\theta)| \leq C|\theta|_\infty\|\theta\|\|\xi_x\| \\ &\leq C\left(\|\theta\|^2 + \|\xi_x\|^2\right).\end{aligned} \tag{61}$$

We conclude from (54)–(61) that

$$|(A_x,\theta)| \leq C\left(N^{2(1-\mu)} + \|\theta\|^2 + \|\xi\|_1^2\right),\ 0 \leq t \leq t_N. \tag{62}$$

We estimate now (θ,ξ_x) and the terms of (B,ξ_x) exactly as in (39)–(44), and conclude that as long as the semidiscrete approximation exists it holds that

$$|(\theta,\xi_x)| + |(B,\xi_x)| \leq C\left(N^{-2\mu} + \|\theta\|^2 + \|\xi\|_1^2\right). \tag{63}$$

Therefore, by (52), (53), (62), (63), since $c', a, d \neq 0$ we see that for $0 \leq t \leq t_N$

$$\frac{1}{2}\frac{d}{dt}\left(\|\theta\|^2 + \|\xi\|_1^2\right) \leq C\left(N^{2(1-\mu)} + \|\theta\|^2 + \|\xi\|_1^2\right).$$

By Gronwall's lemma and (20) we see that for $0 \leq t \leq t_N$ and a constant $C(T)$ there holds

$$\|\theta\| + \|\xi\|_1 \leq C(T)N^{1-\mu}. \tag{64}$$

Therefore, since $|\theta|_\infty \leq CN^{1/2}\|\theta\|$ by (17), and using (64) and the assumption that $\mu > 3/2$, we see that t_N was not maximal in (60) if N was sufficiently large. We conclude that (64) holds up to $t = T$ which implies that

$$\max_{0\leq t\leq T}(\|\zeta_N - \zeta\| + \|u_N - u\|_1) \leq CN^{1-\mu},$$

that is, that the conclusion (49) of the proposition holds. Note that this implies that u_N is optimally close to u in H^1 but ζ_N suboptimally so to ζ in L^2. ∎

Proposition 5. *Let a, b, c, d as in case (iv), and with no loss of generality suppose that $b = 0, d > 0, a = c = 0$. If $\mu > 3/2$ then*

$$\max_{0\leq t\leq T}(\|\zeta_N - \zeta\| + \|u_N - u\|_1) \leq CN^{1-\mu}.$$

Proof. While the semidiscrete solution ζ_N, u_N exists, putting $\varphi = \theta$ in (22), $\chi = \xi$ in (24), and using integration by parts, then adding the resulting equations yields

$$\frac{1}{2}\frac{d}{dt}\left(\|\theta\|^2+\|\xi\|^2+d\|\xi_x\|^2\right)=-\kappa_1(\xi_x,\theta)-(A_x,\theta)+\kappa_2(\theta,\xi_x)+(B,\xi_x).$$

We estimate now the terms of (A_x,θ) and (B,ξ_x) exactly as in Proposition 4. The conclusion follows. ■

Proposition 6. *Let a,b,c,d as in case (v), and with no loss of generality suppose that $b>0,d>0,a=0,c<0$. If $\mu\geq 1$ then*

$$\max_{0\leq t\leq T}(\|\zeta_N-\zeta\|+\|u_N-u\|)\leq CN^{-\mu}.$$

Proof. We write (22) for $a=0$ as

$$\theta_t-b\theta_{xxt}=-\kappa_1\xi_x-PA_x,$$

that is, as

$$(1-b\partial_x^2)\theta_t=-\kappa_1\xi_x-PA_x. \tag{65}$$

For a constant $\kappa>0$ let $\mathcal{T}_\kappa$ denote the operator $\mathcal{T}_\kappa=(I-\kappa\partial_x^2)^{-1}$ which is well defined in H^s for any $s\in\mathbb{R}$. Using its Fourier representation we see, for any $f\in H^{j-2}$, that $\mathcal{T}_\kappa f\in H^j$ and that

$$\|\mathcal{T}_\kappa f\|_j\leq C_k\|f\|_{j-2},\ j\in\mathbb{R}, \tag{66}$$

where C_k is a constant depending on κ. (In the sequel we will only use the property that for $f\in L^2$, $\|f\|_{-j}\leq\|f\|, j\geq 0$, for the negative norms.)

Using this notation, we write (65) as

$$\theta_t=-\kappa_1\mathcal{T}_b\xi_x-\mathcal{T}_bPA_x.$$

Therefore, since ∂_x commutes with $\mathcal{T}_b$ and P, (66) gives

$$\|\theta_t\|_1\leq|\kappa_1|\|\mathcal{T}_b\xi_x\|_1+\|\mathcal{T}_bPA_x\|_1\leq C(\|\xi\|+\|A\|). \tag{67}$$

From the definition of A, compare (23), we see that

$$\begin{aligned}\|A\|\leq C(&|u|_\infty\|\rho\|+|\zeta|_\infty\|\sigma\|+|u|_\infty\|\theta\|+|\zeta|_\infty\|\xi\|\\&+|\sigma|_\infty\|\theta\|+|\rho|_\infty\|\xi\|+|\rho|_\infty\|\sigma\|+\|\theta\||\xi|_\infty).\end{aligned} \tag{68}$$

Since $\xi(0)=0$, using continuity, let $t_N\in(0,T]$ denote the maximal time for which the solution of the semidiscrete IVP exists and satisfies

$$|\xi|_\infty\leq 1,\ 0\leq t\leq t_N. \tag{69}$$

Therefore, from (68), using the fact that $\mu\geq 1$, Sobolev's inequality (15), and (16), we obtain, in view of (69), that

$$\|A\|\leq C(N^{-\mu}+\|\theta\|+\|\xi\|),\ 0\leq t\leq t_N. \tag{70}$$

Hence, from (67) and (70) we get

$$\|\theta_t\|_1\leq C(N^{-\mu}+\|\theta\|+\|\xi\|),\ 0\leq t\leq t_N.$$

We write now (24) as

$$(1-d\partial_x^2)\xi_t=-c'\theta_{xxx}-\kappa_2\theta_x-PB_x,$$

that is, as

$$\xi_t=-c'\mathcal{T}_d\theta_{xxx}-\kappa_2\mathcal{T}_d\theta_x-\mathcal{T}_dPB_x,$$

from which, using (66), we get

$$\begin{aligned}\|\xi_t\| &\le |c'|\|\mathcal{T}_d\theta_{xxx}\| + |\kappa_2|\|\mathcal{T}_d\theta_x\| + \|\mathcal{T}_d PB_x\| \\ &\le C\left(\|\theta\|_1 + \|\theta\| + \|B\|\right) \le C\left(\|\theta\|_1 + \|B\|\right). \end{aligned} \tag{71}$$

From (25) we see that

$$\|B\| \le C\left(|u|_\infty\|\sigma\| + |u|_\infty\|\xi\| + |\sigma|_\infty\|\xi\| + |\sigma|_\infty\|\sigma\| + |\xi|_\infty\|\xi\|\right).$$

Therefore, since $\mu \ge 1$, from (15) and (16), we have, in view of (69), that

$$\|B\| \le C\left(N^{-\mu} + \|\xi\|\right),\ 0 \le t \le t_N. \tag{72}$$

Therefore, by (71) and (72) it follows that

$$\|\theta_t\|_1 + \|\xi_t\| \le C\left(N^{-\mu} + \|\theta\|_1 + \|\xi\|\right),\ 0 \le t \le t_N, \tag{73}$$

where C does not depend on t_N. From (20) we infer that $\theta = \int_0^t \theta_\tau d\tau$, $\xi = \int_0^t \xi_\tau d\tau$. Hence, by (73) we have, for $0 \le t \le t_N$

$$\begin{aligned}\|\theta\|_1 + \|\xi\| &\le \int_0^t \left(\|\theta_\tau\|_1 + \|\xi_\tau\|\right) d\tau \\ &\le C\int_0^t \left(N^{-\mu} + \|\theta\|_1 + \|\xi\|\right) d\tau \\ &\le C\int_0^t \left(\|\theta\|_1 + \|\xi\|\right) d\tau + CTN^{-\mu}.\end{aligned}$$

Using Gronwall's lemma in integral form gives that for some $C = C(T)$

$$\|\theta\|_1 + \|\xi\| \le CN^{-\mu},\ 0 \le t \le t_N. \tag{74}$$

From this we observe, since $\mu \ge 1$, that for $0 \le t \le t_N$ $|\xi|_\infty \le 1$ if N is sufficiently large, and therefore that t_N was not maximal in (69). We may then take $t_N = T$ and conclude from (74) that

$$\|\theta\|_1 + \|\xi\| \le CN^{-\mu},\ 0 \le t \le T.$$

Therefore, the conclusion of the proposition holds. It implies that ζ_N and u_N satisfy optimal-order L^2-error estimates. ■

Proposition 7. *Let a, b, c, d as in case (vi) and $\mu > 3/2$. Then*

$$\max_{0\le t\le T}\left(\|\zeta_N - \zeta\| + \|u_N - u\|_1\right) \le CN^{1-\mu}.$$

Proof. Motivated by an *a priori* estimate for this system in Theorem 3.1 of [6], and putting $\varphi = \theta$ in (22) and using integration by parts we get, while the semidiscrete approximation exists

$$\frac{1}{2}\frac{d}{dt}\|\theta\|^2 = -\kappa_1(\xi_x, \theta) - (A_x, \theta) + a(\xi_{xx}, \theta_x). \tag{75}$$

Now putting $\chi = \xi + a\xi_{xx}$ in (24) and using integration by parts, we get, while the semidiscrete approximation exists,

$$\begin{aligned}\frac{1}{2}\frac{d}{dt}\left(\|\xi\|^2 + (|a| + d)\|\xi_x\|^2 + |a|d\|\xi_{xx}\|^2\right) &= -\kappa_2(\theta_x, \xi) - a\kappa_2(\theta_x, \xi_{xx}) \\ &\quad - (B_x, \xi + a\xi_{xx}).\end{aligned} \tag{76}$$

In order to eliminate the term (ξ_{xx}, θ_x) from (75) and (76) we multiply (75) by $\kappa_2 > 0$ and add the resulting equation to (76). In this way we get

$$\frac{1}{2}\frac{d}{dt}\left(\kappa_2\|\theta\|^2 + \|\xi\|^2 + (|a|+d)\|\xi_x\|^2 + |a|d\|\xi_{xx}\|^2\right) = -\kappa_1\kappa_2(\xi_x,\theta) - \kappa_2(A_x,\theta) - (B_x, \xi + a\xi_{xx}) - \kappa_2(\theta_x,\xi). \quad (77)$$

We now estimate the right-hand side of (77). The terms (ξ_x,θ), (A_x,θ) are estimated as in the proof of Proposition 4. Assuming that t_N is the maximal time in $(0,T]$ for which the semidiscrete approximation exists and satisfies, in view of (20),

$$|\theta|_\infty \le 1, \ \ 0 \le t \le t_N, \quad (78)$$

we see, as in (53) and (62), that for $0 \le t \le t_N$

$$|(\xi_x,\theta)| + |(A_x,\theta)| \le C\left(N^{2(1-\mu)} + \|\theta\|^2 + \|\xi\|_1^2\right). \quad (79)$$

Examining the rest of the terms in the right-hand side of (77) we first note that

$$|(\theta_x,\xi)| = |(\theta,\xi_x)| \le \frac{1}{2}(\|\theta\|^2 + \|\xi_x\|^2). \quad (80)$$

In the last term of the right-hand side of (77) the inner product with ξ is easily estimated by integrating by parts and arguing as in (40)–(44). This gives

$$|(B_x,\xi)| = |(B,\xi_x)| \le C(N^{-2\mu} + \|\xi\|_1^2). \quad (81)$$

We now estimate the terms in the inner product (B_x,ξ_{xx}). We have, since H^1 is an algebra, using (15) and our hypothesis on μ, that

$$|((u\sigma)_x,\xi_{xx})| \le C\|u\|_1\|\sigma\|_1\|\xi_{xx}\| \le C(N^{2(1-\mu)} + \|\xi_{xx}\|^2), \quad (82)$$

$$|((u\xi)_x,\xi_{xx})| \le C\|u\|_1\|\xi\|_1\|\xi_{xx}\| \le C\|\xi\|_2^2, \quad (83)$$

$$|((\sigma\xi)_x,\xi_{xx})| \le C\|\sigma\|_1\|\xi\|_1\|\xi_{xx}\| \le C\|\xi\|_2^2. \quad (84)$$

Since $\mu > 3/2$ we have by (15), (16)

$$|((\sigma^2)_x,\xi_{xx})| \le C|\sigma|_\infty\|\sigma\|_1\|\xi_{xx}\| \le CN^{\frac{3}{2}-2\mu}\|\xi_{xx}\| \le CN^{-\mu}\|\xi_{xx}\| \le C(N^{-2\mu} + \|\xi_{xx}\|^2). \quad (85)$$

Finally, assuming that t_N in (78) is small enough so that in addition to (78) we have

$$|\xi|_\infty \le 1, \ 0 \le t \le t_N, \quad (86)$$

we obtain for $0 \le t \le t_N$

$$|((\xi^2)_x,\xi_{xx})| \le 2|\xi|_\infty\|\xi_x\|\|\xi_{xx}\| \le C\|\xi\|_2^2. \quad (87)$$

From (77), (79)–(85), and (87), since $\kappa_2, d > 0$ we obtain

$$\frac{d}{dt}\left(\|\theta\|^2 + \|\xi\|_2^2\right) \le C(N^{2(1-\mu)} + \|\theta\|^2 + \|\xi\|_2^2), \ \ 0 \le t \le t_N,$$

where the constant C does not depend on t_N. By Gronwall's lemma then, for $0 \le t \le t_N$

$$\|\theta\| + \|\xi\|_2 \le C_T N^{1-\mu}. \quad (88)$$

Since by (17) $|\theta|_\infty \le CN^{1/2}\|\theta\|$, and since $|\xi|_\infty \le C\|\xi\|_1$ by Sobolev's theorem, we see that (88) implies, in view of our assumption on μ, that t_N in (78) and (86) is not maximal if N is sufficiently large, and, as usual, can be taken equal to T. We infer that (88) holds up to $t = T$ and that the conclusion of the proposition follows, giving an optimal-order H^1 error estimate for u_N and a suboptimal-order one for ζ_N in L^2. ∎

Proposition 8. *Let a, b, c, d as in case (vii) and with no loss of generality suppose that $a < 0, b > 0, d = 0, c = 0$. If $\mu > 3/2$, then*

$$\max_{0\le t\le T} (\|\zeta_N - \zeta\| + \|u_N - u\|) \le CN^{1-\mu}. \tag{89}$$

Proof. These systems are of the form

$$\zeta_t + \kappa_1 u_x + \lambda(\zeta u)_x + a u_{xxx} - b\zeta_{xxt} = 0, \tag{90}$$

$$u_t + \kappa_2 \zeta_x + \lambda u u_x = 0. \tag{91}$$

Motivated by an analogous observation in [6], Section 3.3, we write the first pde (90) above in the equivalent form

$$\zeta_t - \frac{a}{b}u_x + (\kappa_1 + \frac{a}{b})\mathcal{T}_b u_x + \lambda\mathcal{T}_b(\zeta u)_x = 0, \tag{92}$$

where $\mathcal{T}_b = (I - b\partial_x^2)^{-1}$ was introduced in the proof of Proposition 6.

Consequently, we will adopt the following semidiscretization of the system: for all $\varphi, \chi \in S_N$

$$(\zeta_{Nt}, \varphi) - \frac{a}{b}(u_{Nx}, \varphi) + \left(\kappa_1 + \frac{a}{b}\right)(\mathcal{T}_b u_{Nx}, \varphi) + \lambda(\mathcal{T}_b(\zeta_N u_N)_x, \varphi) = 0, \tag{93}$$

$$(u_{Nt}, \chi) + \kappa_2(\zeta_{Nx}, \chi) + \lambda(u_N u_{Nx}, \chi) = 0, \tag{94}$$

with

$$\zeta_N(0) = P\zeta_0, u_N(0) = Pu_0. \tag{95}$$

It is clear that the solution of this IVP exists at least locally in time.

We proceed now to the proof of the error estimate (89). While the semidiscrete solution exists, using our usual notation and subtracting the weak form of (92) from (93) we have for all $\varphi \in S_N$

$$(\theta_t, \varphi) - \frac{a}{b}(\xi_x, \varphi) = -\left(\kappa_1 + \frac{a}{b}\right)(\mathcal{T}_b(\xi_x + \sigma_x), \varphi) - \lambda(\mathcal{T}_b A_x, \varphi). \tag{96}$$

From the weak form of (91) and (94) we obtain

$$(\xi_t, \chi) + \kappa_2(\theta_x, \chi) = -\lambda(B_x, \chi), \forall \chi \in S_N. \tag{97}$$

Putting $\varphi = \theta$ in (96), $\chi = \xi$ in (97) gives

$$\frac{1}{2}\frac{d}{dt}\|\theta\|^2 - \frac{a}{b}(\xi_x, \theta) = -\left(\kappa_1 + \frac{a}{b}\right)(\mathcal{T}_b(\xi_x + \sigma_x), \theta) - \lambda(\mathcal{T}_b A_x, \theta),$$
$$\frac{1}{2}\frac{d}{dt}\|\xi\|^2 - \kappa_2(\theta, \xi_x) = -\lambda(B_x, \xi).$$

Multiplying the first equation above by κ_2 and the second by $-a/b$ and adding we get

$$\frac{1}{2}\frac{d}{dt}\left(\kappa_2\|\theta\|^2 + \frac{|a|}{b}\|\xi\|^2\right) = -\kappa_2(\kappa_1 + \frac{a}{b})(\mathcal{T}_b(\xi + \sigma)_x, \theta) - \kappa_2\lambda(\mathcal{T}_b A_x, \theta) + \frac{a}{b}\lambda(B_x, \xi). \tag{98}$$

For the first two terms in the right-hand side of (98) we have, in view of (66)

$$|(\mathcal{T}_b(\xi+\sigma)_x,\theta)| \le \|\mathcal{T}_b(\xi+\sigma)_x\|\|\theta\| \le C(\|\xi\|+\|\sigma\|)\|\theta\|, \tag{99}$$

$$|(\mathcal{T}_b A_x,\theta)| \le \|\mathcal{T}_b A_x\|\|\theta\| \le C\|A\|\|\theta\|. \tag{100}$$

We bound the right-hand side of (99) as usual by

$$(\|\xi\|+\|\sigma\|)\|\theta\| \le C(N^{-2\mu}+\|\xi\|^2+\|\theta\|^2). \tag{101}$$

In order to bound the right-hand side of (100), we argue as in the proof of Proposition 6; in particular, consider (68). The only difference is in the last term of A, which we now bound by $\|\xi\||\theta|_\infty$. Consequently, let t_N, $0 < t_N \le T$ be the maximal time for which the semidiscrete approximation exists and is such that

$$|\theta|_\infty \le 1,\ 0 \le t \le t_N. \tag{102}$$

We therefore obtain, for $0 \le t \le t_N$, that

$$\|A\|\|\theta\| \le C(N^{-2\mu}+\|\theta\|^2+\|\xi\|^2). \tag{103}$$

We now estimate the last term of the right-hand side of (98). Using the definition (25) of B, we have, since H^1 is an algebra and in view of (15), that

$$|((u\sigma)_x,\xi)| \le \|u\|_1\|\sigma\|_1\|\xi\| \le C\|\sigma\|_1\|\xi\| \le C(N^{2(1-\mu)}+\|\xi\|^2). \tag{104}$$

By integrating by parts we see that

$$|((u\xi)_x,\xi)| = \frac{1}{2}|(u_x\xi,\xi)| \le \frac{1}{2}|u_x|_\infty\|\xi\|^2 \le C\|\xi\|^2, \tag{105}$$

using our hypothesis on μ. Similarly, by (16)

$$|((\sigma\xi)_x,\xi)| = \frac{1}{2}|(\sigma_x\xi,\xi)| \le \frac{1}{2}|\sigma_x|_\infty\|\xi\|^2 \le C\|\xi\|^2. \tag{106}$$

By our hypothesis on μ and (15), (16)

$$\begin{aligned}|(\sigma\sigma_x,\xi)| &\le |\sigma|_\infty\|\sigma_x\|\|\xi\| \le CN^{\frac{1}{2}-\mu}N^{1-\mu}\|\xi\| \\ &\le CN^{-\mu}\|\xi\| \le C(N^{-2\mu}+\|\xi\|^2).\end{aligned} \tag{107}$$

And finally, by periodicity

$$(\xi\xi_x,\xi) = 0. \tag{108}$$

By (104)–(108) we conclude, as long as the solution of (93)–(95) exists, that

$$|(B_x,\xi)| \le C(N^{2(1-\mu)}+\|\xi\|^2). \tag{109}$$

Therefore, by (98), since $\kappa_2, b > 0$, and using (99), (101), (103), (109) we have for $0 \le t \le t_N$

$$\frac{d}{dt}\left(\|\theta\|^2+\|\xi\|^2\right) \le C(N^{2(1-\mu)}+\|\theta\|^2+\|\xi\|^2).$$

Hence, by Gronwall's lemma, in view of (95) we obtain for $0 \le t \le t_N$

$$\|\theta\|+\|\xi\| \le C_T N^{1-\mu}. \tag{110}$$

Since $|\theta|_\infty \le CN^{1/2}\|\theta\| \le CN^{3/2-\mu}$ by the above, in view of our hypothesis on μ, and provided we take N sufficiently large, we infer that t_N in (102) was not maximal; as usual, we may take $t_N = T$. Thus (110) holds up to $t = T$, giving (89). This inequality implies that ζ_N and u_N satisfy in this case suboptimal L^2-error estimates. ■

4 | FULL DISCRETIZATION AND NUMERICAL EXPERIMENTS

In this section, we complete the study of the numerical approximation of the B/B systems (5) by introducing a time-stepping scheme for the spectral semidiscrete systems (18), (19). The performance of the resulting fully discrete method is illustrated with some numerical experiments.

4.1 | Temporal discretization of the spectral semidiscrete systems

We consider the periodic initial-value problem (13), (14) on a long enough interval $(-L, L)$ and discretize it in space with the spectral Galerkin method introduced in Section 3. After the change from the interval $(0, 1)$ (for which the convergence analysis was made) to $(-L, L)$ is performed, the corresponding system (18)–(20) is solved in terms of the Fourier coefficients of the semidiscrete approximations in analogy to (21). This leads to an ode system of the form

$$\frac{d}{dt}\begin{pmatrix}\widehat{\zeta_N}\\ \widehat{u_N}\end{pmatrix} = F\begin{pmatrix}\widehat{\zeta_N}\\ \widehat{u_N}\end{pmatrix}, \tag{111}$$

where for $-N \leq k \leq N, \hat{k} = k\pi/L$

$$F\begin{pmatrix}\widehat{\zeta_N}\\ \widehat{u_N}\end{pmatrix}(\hat{k}) = \begin{pmatrix}\frac{1}{1+b\hat{k}^2}\left(i\hat{k}((-\kappa_1 + a\hat{k}^2)\widehat{u_N}(\hat{k},t) - \lambda\widehat{\zeta_N u_N}(\hat{k},t))\right)\\ \frac{1}{1+d\hat{k}^2}\left(i\hat{k}(-\kappa_2(1-c\hat{k}^2)\widehat{\zeta_N}(\hat{k},t) - \frac{\lambda}{2}\widehat{u_N^2}(\hat{k},t))\right)\end{pmatrix}, \tag{112}$$

with $\hat{\zeta}_N(\hat{k},0) = \hat{\zeta}_0(\hat{k}), \hat{u}_N(\hat{k},0) = \hat{u}_0(\hat{k})$. The ode system (111), (112) is then discretized in time with the fourth-order, three-stage RK-composition method based on the implicit midpoint rule (IMR) [20, 33]. The scheme belongs to the family of RK methods with Butcher tableau

$$\begin{array}{c|c} & a_{ij} \\ \hline & b_i \end{array} = \begin{array}{|ccccc} b_1/2 & & & & \\ b_1 & b_2/2 & & & \\ b_1 & b_2 & \ddots & & \\ \vdots & \vdots & & \ddots & \\ b_1 & b_2 & \cdots & \cdots & b_s/2 \\ \hline b_1 & b_2 & \cdots & \cdots & b_s \end{array}, \tag{113}$$

in the particular case of $s = 3$ and

$$b_1 = (2 + 2^{1/3} + 2^{-1/3})/3 = \frac{1}{2 - 2^{1/3}} \sim 1.351,$$
$$b_2 = 1 - 2b_1 \sim -1.702, \quad b_3 = b_1, \tag{114}$$

The method (113), (114) can be written as a composition of three steps of the IMR with stepsizes $b_1\Delta t, b_2\Delta t$, and $b_3\Delta t$. For a general ode system $\dot{y} = f(y)$ this reads

$$y^{n,1} = y^n + b_1\Delta t f\left(\frac{y^n + y^{n,1}}{2}\right),$$
$$y^{n,j} = y^n + b_j\Delta t f\left(\frac{y^{n,j-1} + y^{n,j}}{2}\right), \; j = 2, 3,$$
$$y^{n+1} = y^{n,3}.$$

The scheme is fourth-order accurate, symplectic, symmetric and of easy implementation. The full discretization has been analyzed in [9] in the case of the spectral semidiscretization of the periodic IVP for the KdV equation and its efficiency has been checked in computations with other nonlinear dispersive equations [12, 18]. It has been shown to be L^2-conservative and convergent under suitable CFL conditions in the case of the KdV. Here, in our experiments with the B/B system (13), (14) in the generic case $a, c < 0, b, d > 0$, we also observed that a Courant stability condition of the form $N\Delta t \leq \alpha$ for some $\alpha > 0$ was sufficient to ensure stability and convergence of the fully discrete scheme.

For an integer $M \geq 1$ the corresponding fully discrete approximation at times $t_m = m\Delta t, m = 0, \ldots, M$, where $T = M\Delta t$, is computed in the Fourier space with FFT techniques.

4.2 | Validation of the codes

In this section, we present some numerical evidence in order to validate the full discretization introduced in Section 4.1. The experiments will additionally serve to give confidence to the numerical simulation of stability and interactions of solitary waves to be carried out in the companion paper [13], compare also [14].

In the first experiment we check the temporal order of convergence by simulating with the fully discrete scheme the propagation of an exact solitary wave solution of (5). For particular values of the speed, exact classical solitary waves can be derived by following the arguments used in [8]. If we look for solutions (ζ, v_β) with $v_\beta = B\zeta$ for some constant B, then, substituting into (12) we have

$$\begin{aligned} (c_s - \kappa_1 B)\zeta - (bc_s + aB)\zeta'' &= B\kappa_{\gamma,\delta}\zeta^2 \\ (c_s B - \kappa_2)\zeta - (dc_s B + \kappa_2 c)\zeta'' &= \frac{B^2}{2}\kappa_{\gamma,\delta}\zeta^2. \end{aligned} \tag{115}$$

The existence of a solution ζ of (115) requires then

$$\begin{aligned} 2c_s B - 2\kappa_2 &= c_s B - \kappa_1 B^2 \\ 2dc_s B + 2\kappa_2 c &= bc_s B + aB^2. \end{aligned} \tag{116}$$

If we consider (116) as a linear system for the variables B^2 and $c_s B$, then we have two possibilities:

- If $b - 2d - a(\delta + \gamma) \neq 0$, then (116) has a unique solution from which
$$B^2 = \frac{2\kappa_2(b - 2d - c)}{\kappa_1(b - 2d) - a}, \quad c_s = \frac{1}{B}\frac{2\kappa_2(c\kappa_1 - a)}{\kappa_1(b - 2d) - a}. \tag{117}$$
- If $b - 2d - a(\delta + \gamma) = 0$, then (116) has infinitely many solutions iff $c = a(\delta + \gamma)$; they satisfy
$$c_s = \frac{2\kappa_2 - \kappa_1 B^2}{B}, \tag{118}$$
for $B \neq 0$ arbitrary.

As far as the exact form of the solutions is concerned, differentiating one of the equations of (115) and using (116) we have

$$\mu_1\zeta' - \mu_2\zeta''' = \zeta\zeta', \tag{119}$$

where

$$\mu_1 = \frac{\kappa_2 - \kappa_1 B^2}{\kappa_{\gamma,\delta}B^2}, \ \mu_2 = \frac{(a - b\kappa_1)B^2 + 2b\kappa_2}{2\kappa_{\gamma,\delta}B^2}.$$

Thus, (119) admits solutions of square hyperbolic secant form if $\mu_1\mu_2 > 0$, that is, if

$$(\kappa_2 - \kappa_1 B^2)((a - b\kappa_1)B^2 + 2b\kappa_2) > 0.$$

If this condition is satisfied, then

$$\zeta(x,t) = 3\mu_1 \operatorname{sech}^2\left(\frac{1}{2}\sqrt{\frac{\mu_1}{\mu_2}}(x - c_s t - x_0)\right),$$
$$u(x,t) = (1 - \partial_{xx})v_\beta = B(\zeta(x,t) - \beta\zeta_{xx}(x,t)), \qquad (120)$$

where B and c_s are given by (117) or (118), and $x_0 \in \mathbb{R}$ is arbitrary.

For the first numerical experiment below, we consider the solution of the form (120) corresponding to the parameter values

$$\delta = 0.9, \gamma = 0.5,$$
$$a = -1/3, c = -2/3,$$
$$b = d = \frac{1}{2}\left(\frac{a}{\kappa_1} - c + \frac{1+\gamma\delta}{3\delta(\delta+\gamma)}\right) \approx 0.2918, \qquad (121)$$

and compute the fully discrete approximation up to a final time $T = 100$ on an interval $(-L, L)$ with $L = 256$ and periodic boundary conditions. According to (117), the speed is $c_s \approx 1.0328$ and the amplitude is $\zeta_{\max} \approx 7.9846$. We made two runs with $N = 2048$ and $N = 4096$ (that is with $h = 2L/N = 0.250$

TABLE 1 L^2-errors and temporal convergence rates at $T = 100$ with $L = 256$ and $N = 2048$ ($h = 0.25$) and $N = 4096$ ($h = 0.125$).

Δt	ζ-error	Rate	v_β-error	Rate
$N = 2048$				
1/40	$1.1028E-05$		$7.3309E-06$	
1/80	$6.8977E-07$	3.9989	$4.5852E-07$	3.9989
1/160	$4.3076E-08$	4.0012	$2.8635E-08$	4.0011
$N = 4096$				
1/40	$1.1028E-05$		$7.3309E-06$	
1/80	$6.8977E-07$	3.9989	$4.5852E-07$	3.9989
1/160	$4.2945E-08$	4.0056	$2.8548E-08$	4.0055

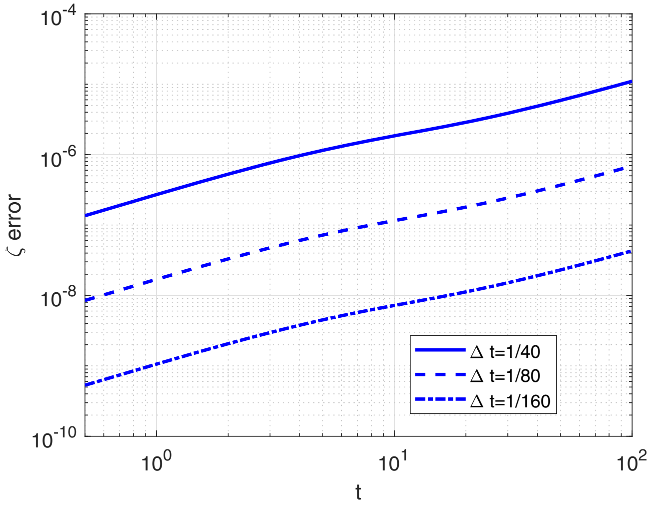

FIGURE 1 Numerical simulation of (5) with the parameter values given in (121) up to $T = 100$ with $N = 4096$. Normalized L^2-error for ζ versus time in log-log scale.

and 0.125 respectively) and several values of Δt. The normalized L^2-errors for ζ and v_β at the final time and the corresponding temporal convergence rates are presented in Table 1. The results show the fourth order of convergence of the time discretization and the associated errors in L^2. Since for the values (121) the system (5) is Hamiltonian (cf. (10)) and its solutions are smooth, decaying to zero at infinity, and preserving the quantities (8) and (9), we may study the ability of the numerical solution to conserve the corresponding discrete versions of the invariants, given by

$$I_h(U,V) = h\sum_{j=0}^{N-1}(U_jV_j + b(D_NU)_j(D_NV)_j), \tag{122}$$

$$E_h(U,V) = h\sum_{j=0}^{N-1}\left(\frac{\kappa_2}{2}U_j^2 + \frac{\kappa_1}{2}V_j^2 - a(D_NV)_j^2 - \kappa_2 c(D_NU)_j^2 + \frac{\kappa_{\gamma,\delta}}{2}U_jV_j^2\right), \tag{123}$$

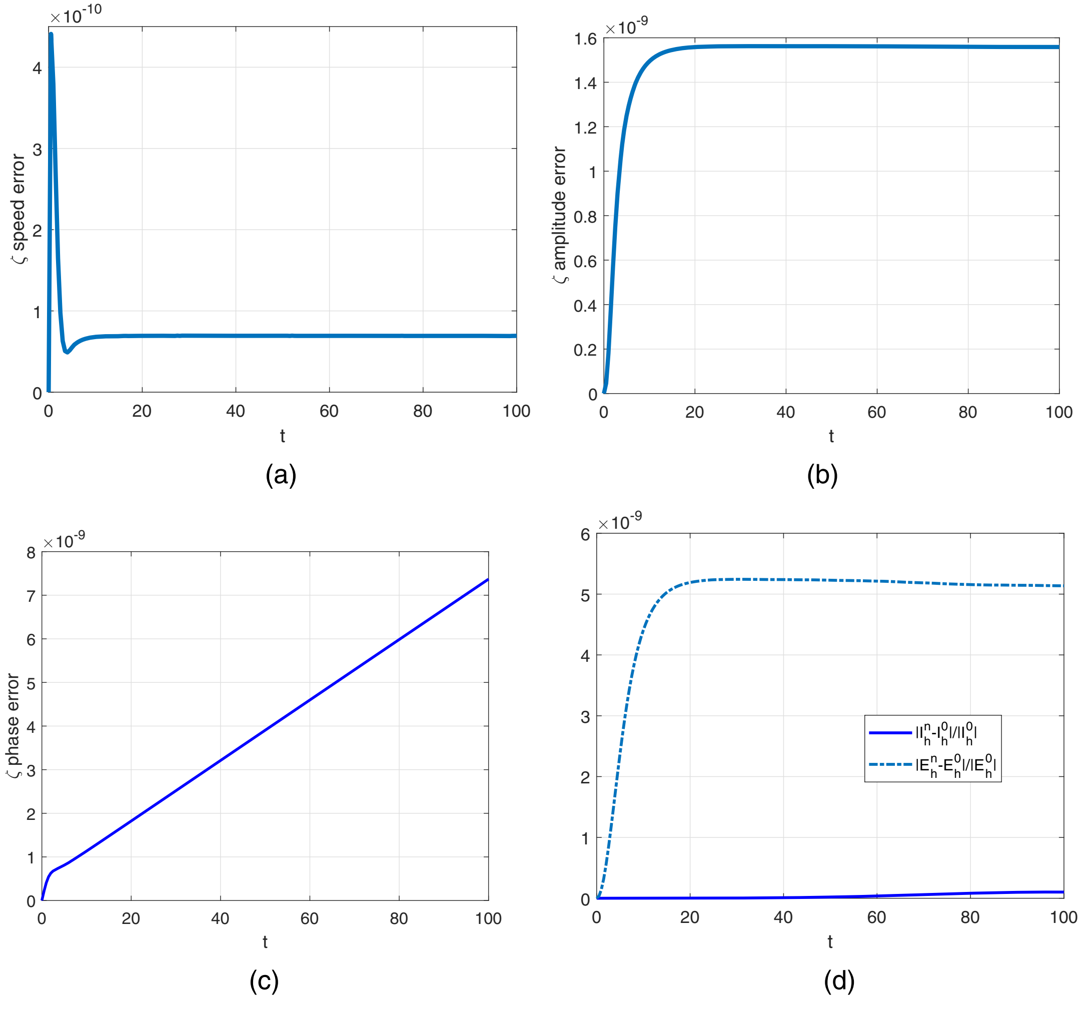

FIGURE 2 Numerical simulation of (5) with the parameter values given in (121) up to $T = 100$ with $N = 4096$. (a) ζ speed error versus time; (b) ζ amplitude error versus time; (c) ζ phase error versus time; (d) errors of discrete quantities (122) and (123) versus time (semilog scale). The errors are normalized and $\Delta t = 1/160$ is taken.

for $U = (U_0, \dots, U_{N-1}), V = (V_0, \dots, V_{N-1})$ and D_N standing for the pseudospectral differentiation matrix of order N. If I_h^n, E_h^n denote, respectively, the values of (122) and (123) evaluated in terms of the numerical solution at time $t_n = n\Delta t$, we obtain the evolution of the normalized errors $|(I_h^n - I_h^0)/I_h^0|, |(E_h^n - E_h^0)/E_h^0|$ shown in Figure 2d for $\Delta t = 1/160$. It suggests the preservation of the two quantities up to the final time $T = 100$ with a normalized error of 1.0198×10^{-10} and 5.1366×10^{-9} respectively. Due to the form of the bilinear invariant (8), we have almost exact in time conservation of the discrete H^1-norm, defined by the pseudospectral differentiation of the numerical solution.

In addition, Figure 1 shows, in log-log scale, the evolution of the normalized ζ errors in L^2 norm as functions of time for $N = 4096$ and several values of Δt. The slopes of the lines suggest approximately linear growth in time of the errors, as expected [19]. A source of this behavior is due to the evolution of the error with respect to some parameters of the solitary waves. For the case at hand this is illustrated by Figure 2a–c showing, for $N = 4096$, $\Delta t = 1/160$, the relative errors in speed, amplitude, and the error in phase, respectively, of the numerical approximation of ζ as functions of time. These errors are computed in a standard way, as for example, in [11]. The results show the preservation of speed and amplitude (up to an error at $t = 100$ of about 6.9340×10^{-11} and 1.5584×10^{-9} respectively) and a

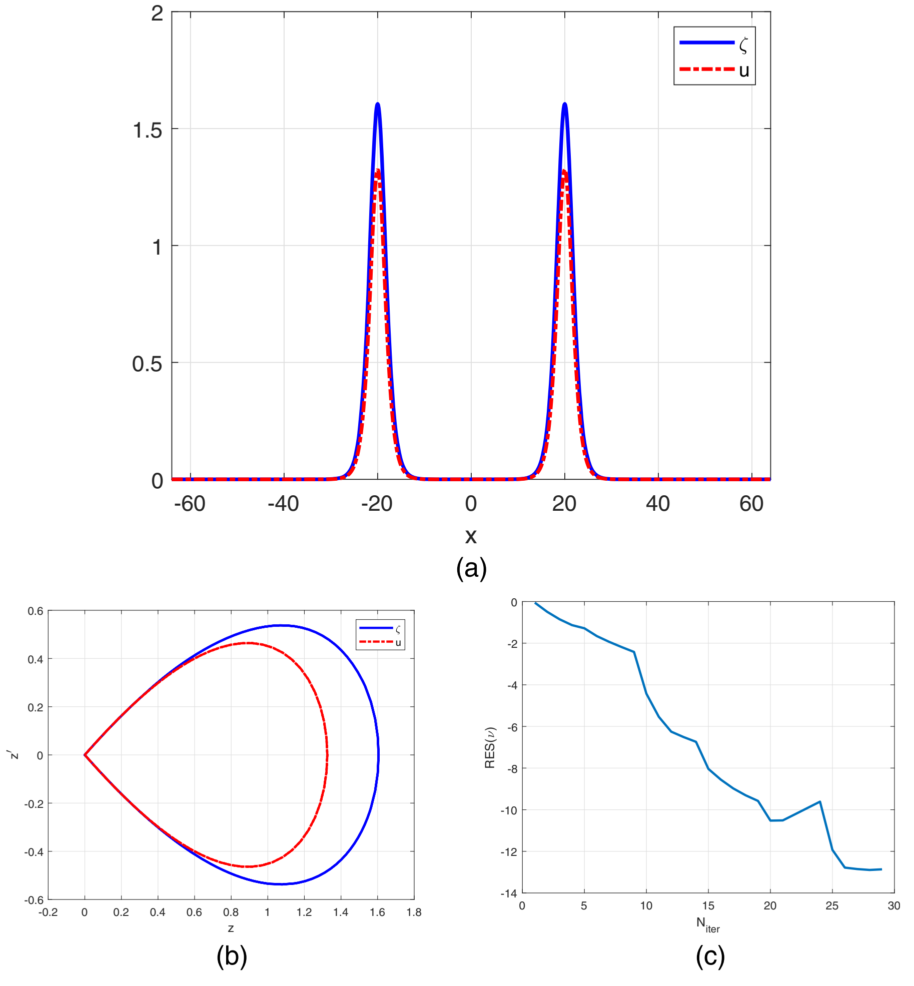

FIGURE 3 Two-pulse solitary wave generated numerically with parameters given by (124). (a) ζ and u profiles; (b) ζ and u phase portraits; (c) residual error versus number of iterations (semilog scale).

linear growth of the phase error. The same experiments were also made with $N = 1024, 2048$. The qualitative results concerning the time behavior of the errors in L^2 norm, in the parameters and in the quantities (122) and (123) were similar and they will not be shown here.

In the second experiment we took the values

$$\delta = 0.9, \gamma = 0.5,\ a = c = 0, b = d = \frac{1}{2}\left(\frac{1+\gamma\delta}{3\delta(\delta+\gamma)}\right) \approx 0.1918, \tag{124}$$

and generated numerically an approximate solution of (12). To this end we followed a standard procedure (cf. e.g., [10, 12] and references therein), consisting on discretizing (12) on $(-L, L)$ with periodic boundary conditions by the Fourier collocation method and solving iteratively the system for the discrete Fourier components of the approximations to the profiles for ζ and v_β by the Petviashvili method [25, 26]. The iterative procedure is in some cases accelerated by using vector extrapolation methods [28-30]. For the application of these techniques to Petviashvili's method for traveling wave computations see [1]. For details of the implementation in the case of the B/B systems, see [13, 14].

In the experiment below, we ran the corresponding iteration taking as initial profile a superposition of two hyperbolic secant square profiles of amplitudes equal to 1 and centered at $x = \pm 20$. The method

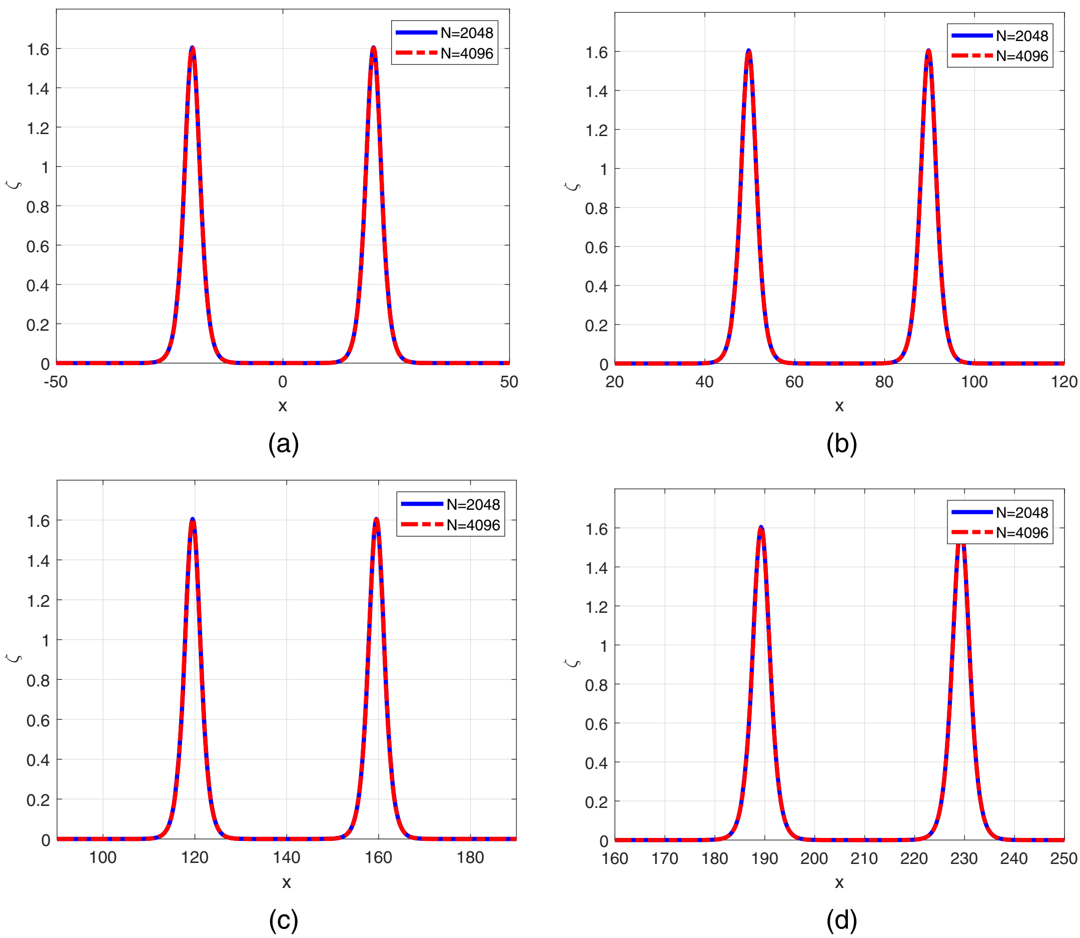

FIGURE 4 Simulation of (5) with parameter values given by (124) up to $T = 400$ with $\Delta t = 1/160$. Approximation of $\zeta(x, t)$ at (a) $t = 0$; (b) $t = 100$; (c) $t = 200$; (d) $t = 300$.

converges to the profile shown in Figure 3, which has the form of a symmetric two-pulse solitary wave. The accuracy of the iteration is first suggested by the convergence to practically zero of the residual error, computed in the standard way [1, 10, 17], and shown in Figure 3c. Both pulses have a computed amplitude of about 1.6055 and the two-pulse wave travels with a speed of 6.9761×10^{-1}.

In addition, we took this computed two-pulse as initial condition of the fully discrete method and monitored the evolution of the numerical solution up to a final time $T = 400$ with several values of the discretization parameters N and Δt. The profiles at several times generated with $\Delta t = 1/160$ and $N = 2048, 4096$, are shown in Figure 4 (note the changing x-axis); they coincide within graph thickness, confirming the ability of the code to simulate classical solitary waves accurately.

The third experiment for checking the accuracy of the codes concerns the simulation of a generalized solitary wave. Taking the values $L = 256$, and

$$\delta = 0.9, \gamma = 0.5,$$
$$a = c = -1/3, b = 0, d = -\frac{a}{\kappa_1} - c + \frac{1+\gamma\delta}{3\delta(\delta+\gamma)} \approx 1.1836, \tag{125}$$

the numerical procedure described above generates generalized solitary-wave (GSW) profile, shown in Figure 5a. (In [13] and [14] we have proved the existence of such solitary waves for systems with

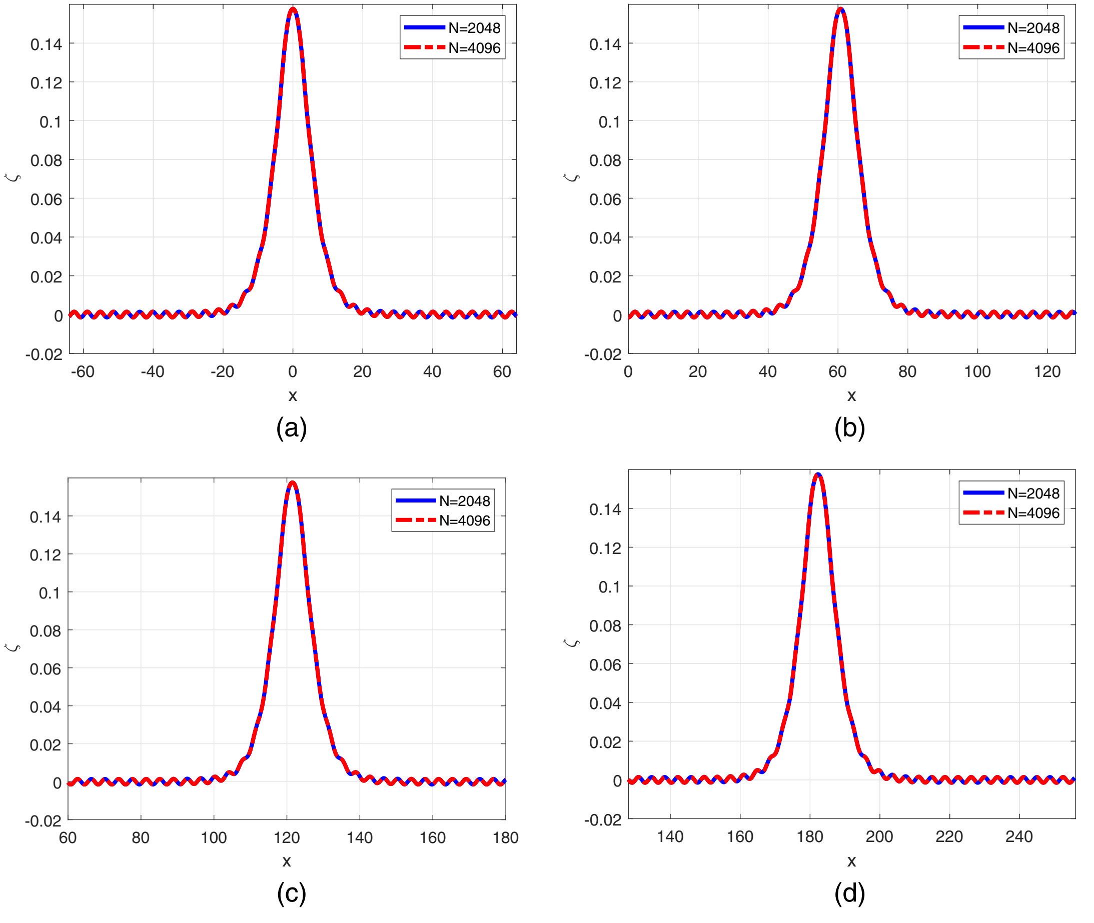

FIGURE 5 Simulation of (5) with parameter values given by (125) up to $T = 400$ with $\Delta t = 1/160$. Approximation of $\zeta(x,t)$ at (a) $t = 0$; (b) $t = 100$; (c) $t = 200$; (d) $t = 300$.

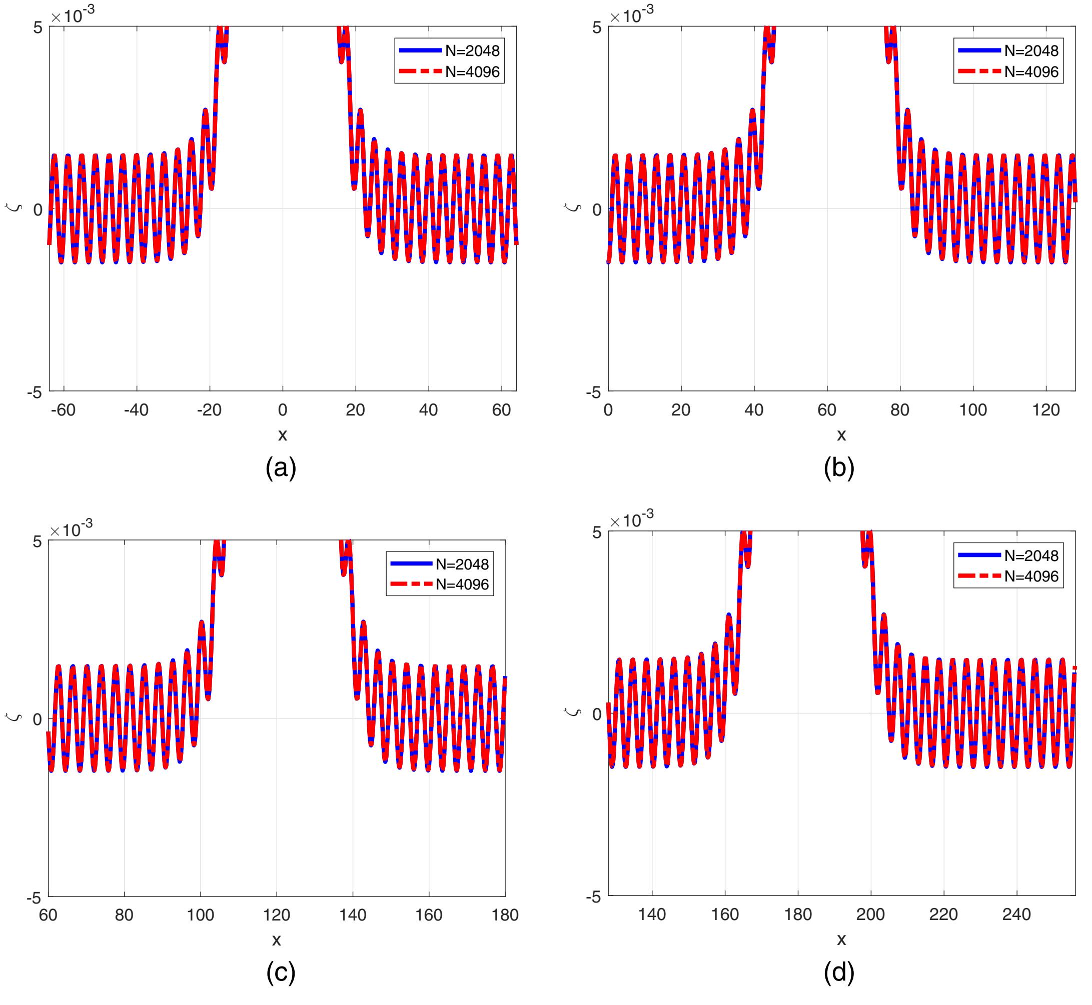

FIGURE 6 Magnification of Figure 5 near the base of the main pulse. Approximation of $\zeta(x,t)$ at (a) $t = 0$; (b) $t = 100$; (c) $t = 200$; (d) $t = 300$.

parameters such as those in (125).) This profile was taken as initial condition for the fully discrete scheme. The evolution of the resulting numerical approximation is observed in the figures that follow. Figure 5b–d shows the numerical approximation of ζ at several time instances with $N = 2048$ and $\Delta t = 1/160$, confirming the preservation of the permanent form of the wave as it evolves. (The amplitude of the computed initial GSW profile is $\zeta_{\max} \approx 1.5764 \times 10^{-1}$ and the profile was generated with speed $c_s = c_{\gamma,\delta} + 0.01 \approx 6.0761 \times 10^{-1}$, where $c_{\gamma,\delta} = \sqrt{(1-\gamma)/(\gamma+\delta)}$ is the associated speed of sound.) The profiles obtained with $N = 4096$ were also computed and they coincide with the corresponding ones obtained for $N = 2048$ within the graph thickness. Figure 6 is a magnification of Figure 5 and shows the structure of the ripples in more detail.

The accuracy of this computation may be also confirmed by considering the evolution of amplitude and speed errors, shown in Figure 7. Observe that this case is not Hamiltonian and the quantities (8), (9) are not preserved by the solution. On the other hand, the L^2 norm of the numerical solution for $N = 2048, 4096$, evaluated at several time instances is shown in Table 2. It is equal to $4.5789161770 \times 10^{-1}$ and is preserved up to twelve digits. This furnishes more evidence of the accuracy of the computations.

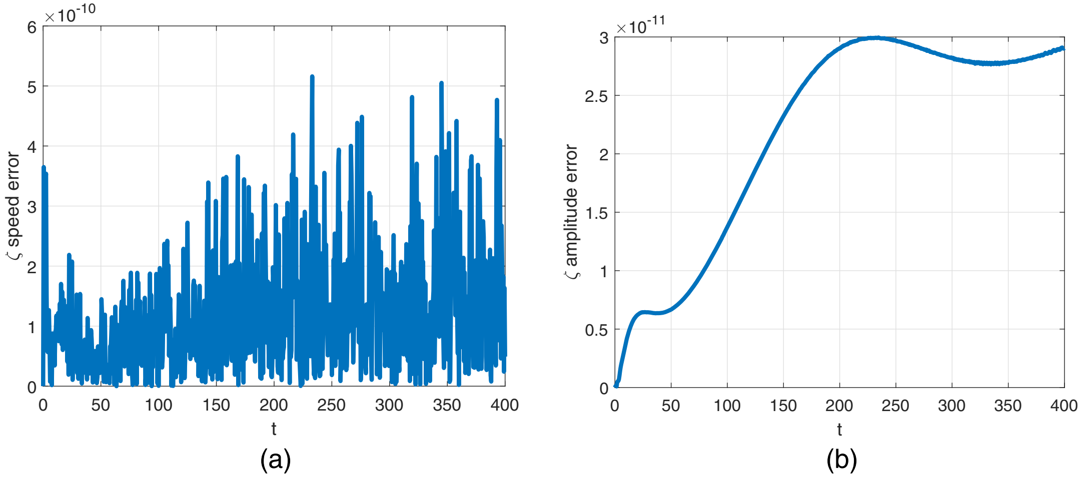

FIGURE 7 Simulation of (5) with parameter values given by (125) up to $T = 400$ with $\Delta t = 1/160$ and $N = 4096$. (a) Normalized ζ speed error versus time; (b) normalized ζ amplitude error versus time.

TABLE 2 Simulation of (5) from a GSW (Figure 5) up to $T = 400$ with $\Delta = 1/160$.

t	$N = 2048$	$N = 4096$
$t = 0$	$4.578916177071256e - 01$	$4.578916177063826e - 01$
$t = 100$	$4.578916177071556e - 01$	$4.578916177064732e - 01$
$t = 200$	$4.578916177072831e - 01$	$4.578916177066413e - 01$
$t = 300$	$4.578916177073125e - 01$	$4.578916177067275e - 01$
$t = 400$	$4.578916177075660e - 01$	$4.578916177070251e - 01$

Note: L^2 norm of ζ component.

5 | CONCLUDING REMARKS

The present paper is concerned with the three-parameter family of internal-wave B/B systems (5). They model the bi-directional propagation of internal waves along the interface of a two-layer system of fluids under a rigid-lid assumption for the upper layer and over a rigid bottom bounding the lower layer below. The systems are derived in [7] under the hypothesis that the flow is in the Boussinesq regime in both layers and are described by four parameters, a, b, c, d, three of them independent, like those corresponding to surface wave propagation [5, 6].

In Section 2 several theoretical issues about this family of systems are discussed. First, the theory developed in [5] for the case of surface waves is used to establish linear and nonlinear well-posedness of the internal-wave systems. Specifically, the B/B systems are linearly well-posed when $a, c \leq 0, b, d \geq 0$. As for local nonlinear well-posedness, an analysis similar to the one in [6] establishes seven types of systems, depending on the parameters a, b, c, d, in corresponding Sobolev spaces where existence, uniqueness and regularity locally in time of solutions hold. They correspond to the cases (i)–(vii) in Section 2.1. When $b = d$ these systems admit a Hamiltonian structure; the Hamiltonian and other conserved quantities are derived in Section 2.2.

Section 3 is devoted to the error analysis of the spectral semidiscretization for approximating the periodic IVP for the B/B systems. Error estimates for the semidiscrete schemes are derived for each cases (i)–(vii) of the nonlinearly well-posed systems.

In Section 4, we integrate numerically in time the spectral semidiscrete systems with a fourth-order RK-composition method based on the implicit midpoint rule, which was previously shown to be accurate and stable for approximating other nonlinear dispersive equations. The accuracy and performance of the resulting full discretization were checked in various numerical experiments involving exact and approximate solitary-wave solutions of (5). In the companion paper [13], compare also [14], we study theoretically the existence of solitary-wave solutions, analyze their numerical generation in more detail, and examine computationally some aspects of their dynamics using the fully discrete procedure introduced here.

ACKNOWLEDGMENTS

The authors are supported by the Spanish Agencia Estatal de Investigación under Research Grant PID2020-113554GB-I00/AEI/10.13039/501100011033. They would like to acknowledge travel support, that made possible this collaboration, from the Institute of Applied and Computational Mathematics of FORTH and the Institute of Mathematics (IMUVa) of the University of Valladolid. Angel Durán is also supported by the Junta de Castilla y León and FEDER funds (EU) under Research Grant VA193P20. Leetha Saridaki is also supported by the Grant "Innovative Actions in Environmental Research and Development (PErAn)" (MIS5002358), implemented under the "Action for the strategic development of the Research and Technological sector" funded by the Operational Program "Competitiveness, and Innovation" (NSRF 2014-2020) and co-financed by Greece and the EU (European Regional Development Fund). The Grant was issued to the Institute of Applied and Computational Mathematics of FORTH.

DATA AVAILABILITY STATEMENT

My manuscript has no associated data.

ORCID

Angel Duran https://orcid.org/0000-0002-6001-3829

REFERENCES

[1] J. Alvarez and A. Duran, *Petviashvili type methods for traveling wave computations: II. Acceleration with vector extrapolation methods*, Math. Comput. Simul. 123 (2016), 19–36.

[2] C. T. Anh, *On the Boussinesq/Full dispersion systems and Boussinesq/Boussinesq systems for internal waves*, Nonlinear Anal. Theory Method Appl. 72 (2010), 409–429.

[3] D. C. Antonopoulos and V. A. Dougalis, *Error estimates for Galerkin approximations of the 'classical' Boussinesq system*, Math. Comp. 82 (2013), 680–717.

[4] D. C. Antonopoulos, V. A. Dougalis, and D. E. Mitsotakis, *Numerical solution of Boussinesq systems of the Bona-Smith family*, Appl. Numer. Math. 60 (2010), 314–336.

[5] J. L. Bona, M. Chen, and J.-C. Saut, *Boussinesq equations and other systems for small-amplitude long waves in nonlinear dispersive media: I. Derivation and linear theory*, J. Nonlinear Sci. 12 (2002), 283–318.

[6] J. L. Bona, M. Chen, and J.-C. Saut, *Boussinesq equations and other systems for small-amplitude long waves in nonlinear dispersive media: II. The nonlinear theory*, Nonlinearity 17 (2004), 925–952.

[7] J. L. Bona, D. Lannes, and J. C. Saut, *Asymptotic models for internal waves*, J. Math. Pures Appl. 89 (2008), 538–566.

[8] M. Chen, *Exact traveling-wave solutions to bi-directional wave equations*, Int. J. Theory Phys. 37 (1998), 1547–1567.

[9] V. A. Dougalis and A. Durán, *A high order fully discrete scheme for the Korteweg-de Vries equation with a time stepping procedure of Runge-Kutta composition type*, IMA J. Numer. Anal. 42 (2022), 3022–3057.

[10] V. A. Dougalis, A. Durán, and D. E. Mitsotakis, *Numerical approximation of solitary waves of the Benjamin equation*, Math. Comput. Simul. 127 (2016), 56–79.

[11] V. A. Dougalis, A. Durán, M. A. López-Marcos, and D. E. Mitsotakis, *A numerical study of the stability of solitary waves of the Bona-Smith family of Boussinesq systems*, J. Nonlinear Sci. 17 (2007), 569–607.
[12] V. A. Dougalis, A. Durán, and D. E. Mitsotakis, *Numerical approximation to Benjamin-type equations. Generation and stability of solitary waves*, Wave Motion 85 (2019), 34–56.
[13] V. A. Dougalis, A. Durán, and L. Saridaki, *On solitary-wave solutions of Boussines/Boussinesq systems for internal waves*, Physica D 428 (2021), 133051.
[14] V. A. Dougalis, A. Durán, and L. Saridaki. *Notes on the numerical analysis and solitary wave solutions of Boussinesq/Boussinesq systems for internal waves*, 2020. http://arxiv.org/abs/2012.07992.
[15] V. A. Dougalis, D. E. Mitsotakis, and J.-C. Saut, *On some Boussinesq systems in two space dimensions: Theory and numerical analysis*, ESAIM Math. Model. Numer. Anal. 41 (2007), 825–854.
[16] V. Duchêne, *Boussinesq-Boussinesq systems for internal waves with a free surface, and the KdV approximation*, ESAIM Math. Model. Numer. Anal. 46 (2012), 145–185.
[17] A. Durán, "On a nonlocal Boussinesq system for internal wave propagation," *Recent advances in differential equations and applications*, J. L. G. Guirao, J. A. Murillo, and F. Periago (eds.), Springer, Cham, 2019, pp. 121–139.
[18] J. de Frutos and J. M. Sanz-Serna, *An easily implementable fourth-order method for the time integration of wave problems*, J. Comput. Phys. 103 (1992), 160–168.
[19] J. de Frutos and J. M. Sanz-Serna, *Accuracy and conservation properties in numerical integration: the case of the Korteweg-de Vries equation*, Numer. Math. 75 (1997), 421–445.
[20] E. Hairer, C. Lubich, and G. Wanner, *Geometric numerical integration, structure-preserving algorithms for ordinary differential equations*, Springer-Verlag, New York, 2004.
[21] E. Lombardi, *Homoclinic orbits to small periodic orbits for a class of reversible systems*, Proc. R. Soc. Edinb. A Math. 126 (1996), 1035–1054.
[22] E. Lombardi, *Homoclinic orbits to exponentially small periodic orbits for a class of reversible systems: application to water waves*, Arch. Ration. Mech. Anal. 137 (1997), 227–304.
[23] E. Lombardi, *Oscillatory integrals and phenomena beyond all algebraic orders*, Springer-Verlag, Berlin, 2000.
[24] H. Y. Nguyen and F. Dias, *A Boussinesq system for two-way propagation of interfacial waves*, Physica D 237 (2008), 2365–2389.
[25] D. E. Pelinovsky and Y. A. Stepanyants, *Convergence of Petviashvili's iteration method for numerical approximation of stationary solutions of nonlinear wave equations*, SIAM J. Numer. Anal. 42 (2004), 1110–1127.
[26] V. I. Petviashvili, *Equation of an extraordinary soliton*, Sov. J. Plasma Phys. 2 (1976), 257–258.
[27] J.-C. Saut, *Asymptotic models for surface and internal waves, 29° Colóquio Brasileiro de Matemática*, IMPA, Rio de Janeiro, 2013.
[28] A. Sidi, *Vector extrapolation methods with applications*, SIAM, Philadelphia, 2017.
[29] A. Sidi, W. F. Ford, and D. A. Smith, *Acceleration of convergence of vector sequences*, SIAM J. Numer. Anal. 23 (1986), 178–196.
[30] D. A. Smith, W. F. Ford, and A. Sidi, *Extrapolation methods for vector sequences*, SIAM Rev. 29 (1987), 199–233.
[31] Y. Ucar, A. Esen, and B. Karaagac, *Numerical solutions of Boussinesq equation using Galerkin finite element method*, Numer. Methods Partial Differ. Equ. 37 (2021), no. 2, 1612–1630.
[32] J. C. Xavier, M. A. Rincon, D. G. Alfaro Vigo, and D. E. Amundsen, *Stability analysis for a fully discrete spectral scheme for Boussinesq systems*, Appl. Anal. 97 (2018), 610–632.
[33] H. Yoshida, *Construction of higher order symplectic integrators*, Phys. Lett. A 150 (1990), 262–268.

How to cite this article: V. A. Dougalis, A. Duran, and L. Saridaki, *On the numerical approximation of Boussinesq/Boussinesq systems for internal waves*, Numer. Methods Partial Differ. Eq. (2023), 1–28. https://doi.org/10.1002/num.23021